Vol. 41 — N° 3 09 17 p. 335 – 358

GEOSTANDARDS and GEOANALYTICAL RESEARCH

A New Appraisal of Sri Lankan BB Zircon as a Reference Material for LA-ICP-MS U-Pb Geochronology and Lu-Hf Isotope Tracing

Maristella M. **Santos** (1, 2)*, Cristiano **Lana** (1), Ricardo **Scholz** (1), Ian **Buick** (3), Mark D. **Schmitz** (4), Sandra L. **Kamo** (5), Axel **Gerdes** (6), Fernando **Corfu** (7), Simon **Tapster** (8), Penelope **Lancaster** (9), Craig D. **Storey** (9), Miguel A.S. **Basei** (10), Eric **Tohver** (11), Ana **Alkmim** (1), Herminio **Nalini** (1), Klaus **Krambrock** (12), Cristiano **Fantini** (12) and Michael **Wiedenbeck** (13)

(1) Applied Isotope Research Group, Departamento de Geologia, Escola de Minas, Universidade Federal de Ouro Preto, Campus Universitário Morro do Cruzeiro s/n, 35400-000, Ouro Preto, MG, Brazil
(2) Instituto Federal de Minas Gerais (IFMG), Campus Congonhas, Minas Gerais, 36415000, Brazil
(3) Department of Earth Sciences, Centre for Crustal Petrology, Stellenbosch University, Private Bag X1, Matieland, 7602, Stellenbosch, South Africa
(4) Department of Geosciences, Boise State University, 1910 University Drive, Boise, ID, 83725, USA
(5) Jack Satterly Geochronology Laboratory, Department of Earth Sciences, University of Toronto, 22 Russell St., Toronto, ON, M5S 3B1, Canada
(6) Institute of Geosciences, Johann Wolfgang Goethe University, Altenhöferallee 1, D-60438, Frankfurt am Main, Germany
(7) Department of Geosciences, University of Oslo, Postbox 1047 Blindern, N-0316, Oslo, Norway
(8) NERC Isotope Geosciences Laboratory, British Geological Survey, Kingsley Dunham Centre, Keyworth, Nottingham, NG12 5GG, UK
(9) School of Earth and Environmental Sciences, Burnaby Building, University of Portsmouth, Portsmouth, PO1 3QL, UK
(10) Centro de Pesquisas Geocronológicas – CPGeo/IGc – USP, São Paulo, SP, Brazil
(11) Tectonics Special Research Centre, University of Western Australia, Perth, WA, Australia
(12) Departamento de Física, Universidade Federal de Minas Gerais, 31.270-901, Belo Horizonte, MG, Brazil
(13) Deutsches GeoForschungsZentrum, Telegrafenberg, 14473, Potsdam, Germany
* Corresponding author. e-mail: maristella.santos@hotmail.com

A potential zircon reference material (BB zircon) for laser ablation-inductively coupled plasma-mass spectrometry (LA-ICP-MS) U-Pb geochronology and Hf isotope geochemistry is described. A batch of twenty zircon megacrysts (0.5–1.5 cm^3) from Sri Lanka was studied. Within-grain rare earth element (REE) compositions are largely homogeneous, albeit with some variation seen between fractured and homogeneous domains. Excluding fractured cathodoluminescence bright domains, the variation in U content for all analysed crystals ranged from 227 to 368 $\mu g\ g^{-1}$ and the average Th/U ratios were between 0.20 and 0.47. The Hf isotope composition (0.56–0.84 g/100 g Hf) is homogeneous within and between the grains – mean $^{176}Hf/^{177}Hf$ of 0.281674 ± 0.000018 (2*s*). The calculated alpha dose of 0.59 × 10^{18} g^{-1} for a number of BB grains falls within the trend of previously studied, untreated zircon samples from Sri Lanka. Aliquots of the same crystal (analysed by ID-TIMS in four different laboratories) gave consistent U-Pb ages with excellent measurement reproducibility (0.1–0.4% RSD). Interlaboratory assessment (by LA-ICP-MS) from individual crystals returned results that are within uncertainty equivalent to the TIMS ages. Finally, we report on within- and between-grain homogeneity of the oxygen isotope systematic of four BB crystals (13.16‰ VSMOW).

Keywords: BB zircon, Sri Lankan reference material, U-Pb geochronology, Hf isotope system, rare earth elements, LA-ICP-MS.

Received 30 Jun 16 – Accepted 04 Feb 17

Zircon, of the available accessory phases used for U-Pb geochronology, has the greatest utility because of its occurrence in a wide range of sedimentary, igneous and metamorphic rock types, its great resistance to weathering, its low initial common Pb uptake and low Pb diffusivity (e.g., Speer 1982, Cherniak and Watson 2003). Hafnium substitution into the zircon lattice up to g/100 g mass fractions (rarely less than 0.3–0.5 g/100 g of Hf) makes it effective for

doi: 10.1111/ggr.12167

tracking crustal evolution in magmatic rocks and fingerprinting detrital zircon populations through its composition. Additionally, the oxygen isotope composition in zircon is robust even through metamorphism and can be used as a petrogenetic tracer (e.g., Valley 2003). The low diffusivity of elements within the zircon lattice (Cherniak and Watson 2003) means that individual zircon crystals commonly preserve multiple compositional and (U-Th-Pb, Hf and O) isotope domains, even after having experienced magmatic and/or high-temperature metamorphic cycles. Analysis of intercrystal domains requires high-spatial resolution analytical approaches such as SIMS (secondary ionisation mass spectrometry) or LA-ICP-MS (laser ablation-inductively coupled plasma-mass spectrometry) to unravel complex zircon growth histories.

The increasingly widespread use of instruments capable of high-spatial resolution isotopic analysis through destructive methods is driving the development of new matrix-matched reference materials for U-Pb geochronology and isotope geochemistry in general. Zircon has also been used, with variable degrees of success, as the calibrant for non-matrix-matched dating of other accessory phases, for which U-Pb reference materials are difficult to obtain, or do not exist (e.g., xenotime, cassiterite, columbite–tantalite, scheelite, perovskite; Gulson and Jones 1992, Batumike *et al.* 2008, Dewaele *et al.* 2011, ZhiChao *et al.* 2011). Natural zircons must be used because of the difficulty in inserting Pb into synthetic crystals (e.g., Wiedenbeck *et al.* 1995, Black *et al.* 2003, Jackson *et al.* 2004, Nasdala *et al.* 2008, Sláma *et al.* 2008). It is important to realise that some level of natural variation is expected and observed within all reference materials and the level of characterisation is in part a function of the number/scale of characterisation experiments, which in the case of this work is exceptionally large and employs multiple independent laboratory techniques.

There are a number of natural zircons used as reference materials for geochronology and isotope geochemistry, including 91500 (megacrysts probably from a syenitic pegmatite; Wiedenbeck *et al.* 1995), Mud Tank (megacrysts from a carbonatite; Woodhead and Hergt 2005), GJ-1 (African Pegmatite; Jackson *et al.* 2004, Morel *et al.* 2008), M257 (Sri Lankan megacryst; Nasdala *et al.* 2008), Temora (~ 200 μm × 100 μm zircons sourced from a monzodiorite; Black *et al.* 2003) and Plešovice (megacrysts from an alkaline granulite; Sláma *et al.* 2008). This study presents isotopic data for natural zircon material that appears to be a suitable reference material for U-Pb dating and Hf isotope measurements by LA-ICP-MS. Our analyses focused on the determination of reliable values of U-Pb age, Hf isotope ratios, REE, U and Hf mass fractions.

Geological background and sample description

The zircon samples for this study come from a placer deposit of the Ratnapura gemstone field (Dissanayake and Rupasinghe 1993), located in the south-western region of the Sri Lankan Highland Complex (Kröner *et al.* 1994b). The Highland Complex is composed of mafic and quartzofeldspathic granulites, charnockitic rocks, marble and quartzite, all metamorphosed to high- and ultrahigh-temperature granulite facies conditions (Kröner *et al.* 1994b, Dissanayake *et al.* 2000, Sajeev *et al.* 2010). Extensive U-Pb isotope studies, including the application of high-spatial resolution techniques such as sensitive high mass resolution ion microprobe (SHRIMP) analysis, have contributed towards establishing a geochronological framework for the high-grade rocks of Sri Lanka (e.g., Hölzl *et al.* 1994, Kröner *et al.* 1994a, Nasdala *et al.* 2004, Sajeev *et al.* 2010, Santosh *et al.* 2014, Dharmapriya *et al.* 2015). In particular, geochronological data have shown that the Highland Complex experienced a prolonged/polyphase granulite facies history from *ca.* 580 to 530 Ma.

Circa 300 g of zircon megacrysts, comprising some eighty grains and hereafter referred as to as the Blueberry (BB) zircons, were acquired and numbered for the present study. We have selected twenty individual crystals (comprising 110 g) of this lot that are dark purple in colour, translucent and commonly larger than 10 mm (Figure 1a, c). The largest (> 10 mm wide) megacrysts (BB9, BB12 and BB17) were broken into hundreds of small (1–2 mm wide) inclusion-free fragments that show only weak oscillatory zoning in cathodoluminescence (CL) images (Figure 2a). A small subset of these BB fragments is, however, marked by fractured domains (e.g., Figure 1b, c) and patchy CL zoning (Figure 2b, c). These domains are commonly associated with inclusions and small (> 10 μm) internal dissolution pits. Five other megacrysts (BB2, BB11, BB13, BB25 and BB39) were sectioned by polishing to reveal internal features (e.g., Figures 1c and 2b). Most parts of such megacrysts are homogeneous, or show only weak CL zoning, or show small domains or rims that are rather bright under CL imaging (e.g., Figure 2b). Other megacrysts such as BB25 showed large domains with a number of fractures, pits and minor mineral inclusions (Figure 2b). Fractures are common around the rims and are often filled with recrystallised zircon (Figure 2c). These domains were excluded from further characterisation.

Analytical methods

Previous studies have established key requirements for minerals such as zircon to be considered as reference

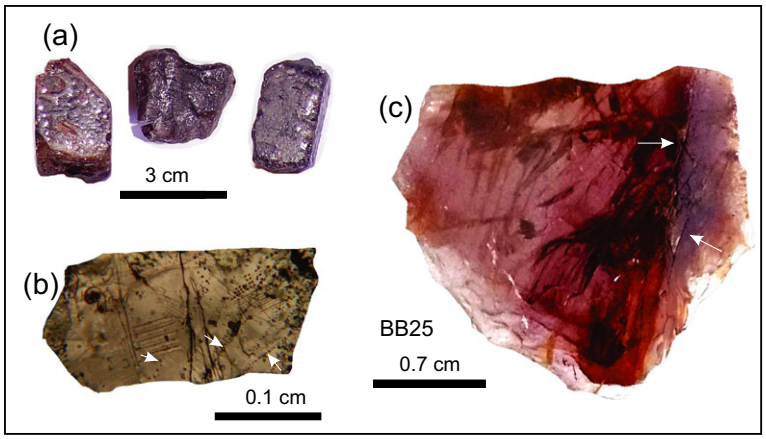

Figure 1. (a) BB zircons with colour and subhedral shapes. (b) Transmitted light image of a small fragment of BB17 showing fracture zones, a small pit and inclusions (white arrows). (c) Whole-grain imaging via transmitted light of BB25 showing fractured domain (white arrows).

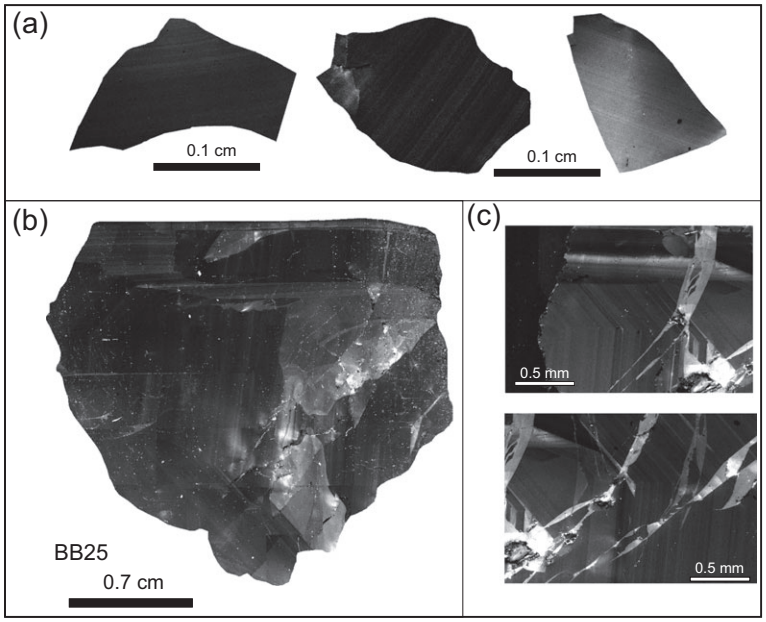

Figure 2. (a) Cathodoluminescence (CL) images of fragments of BB megacrysts (grains BB9, BB12 and BB17), showing rather homogeneous domains marked by thin/weak oscillatory zoning. (b) Whole-grain CL imaging of BB25 showing homogeneous, low CL domains and bright, fractured domains. For comparison, note that light cathodoluminescence correlates with a high density of fractures (right portion of BB25) shown in Figure 1b. (c) Detailed CL image of fractured domains of BB12 – note that fractures have been sealed with recrystallised zircon.

materials for U-Pb and Hf isotope determinations by LA-ICP-MS (e.g., Wiedenbeck *et al.* 1995, 2004, Black *et al.* 2003, Jackson *et al.* 2004, Sláma *et al.* 2008, Li *et al.* 2010, Gonçalves *et al.* 2016). First, the mineral must be dated with high precision and accuracy by independent methods, and there must be limited variability in both U-Pb age and Hf isotope composition. Furthermore, moderate U (tens to hundreds $\mu g\ g^{-1}$) and adequate Hf (a few per cent) contents, low common Pb as well as low Lu/Hf and Yb/Hf ratios are desirable. With respect to oxygen isotope characteristics, demonstrable homogeneity at the nanogram sampling level at uncertainty levels is better than offered by

microanalytical methods (i.e., ± 0.2‰ (2*s*) or better). The material should be sufficiently large for repeated analyses by laser ablation (grains several millimetres to centimetres in diameter) and should be available in large quantities for distribution to the scientific community and for enabling data traceability between analytical facilities.

To ensure extensive characterisation of the zircon investigated in this study, chemical and isotopic analyses were conducted using a number of different techniques (Table 1) in several laboratories: *ID-TIMS*: Jack Satterly Geochronology Laboratory (JSGL; Canada), NERC Isotope Geosciences Laboratory (NIGL; UK), University of Oslo (Norway), Boise State University (BSU; USA); *U-Pb LA-ICP-MS*: J.W. Goethe University of Frankfurt am Main (JWG; Germany), Federal University of Ouro Preto (UFOP; Brazil), University of Portsmouth (UK), University of São Paulo (USP; Brazil); *Trace Element LA-ICP-MS*: UFOP (Brazil); Lu-Hf isotope *LA-ICP-MS*: JWG (Germany), UFOP (Brazil); *Cathodoluminescence imaging*: UFOP (Brazil); *Raman spectroscopy*: Federal University of Minas Gerais (UFMG; Brazil); and *X-ray powder diffraction*: UFOP (Brazil). Where possible, the measurements were reproduced by similar techniques in different laboratories. See Table 1 for a full summary of the methods employed on the twenty BB crystals.

For the characterisation of U-Th-Pb systematics, fragments of the BB crystals were selected and distributed to various TIMS and LA-ICP-MS laboratories. Some of the largest fragments were distributed only to LA-ICP-MS laboratories (Table 1). The key objective here was to perform a blind test to assess age variations between and within individual grains. For details of the methods and instrumentation, see online supporting information Appendix S1.

With respect to our investigation of the isotope systematics of the BB sample suite, a mount was prepared that contained two or three fragments from each of the crystals BB9, BB12, BB25 and BB39. Furthermore, the same epoxy mount included the zircon reference materials 91500, Temora 2 (Black *et al.* 2004), Plešovice and Penglai (Li *et al.* 2010) (Appendix S2). A Cameca 1280-HR SIMS instrument located at the Deutsches GeoForschungsZentrum (GFZ), Potsdam was used to conduct a total of 227 $^{18}O^-/^{16}O^-$ determinations during a 17-h period run in fully automated mode. The SIMS instrumental set-up followed that of Nasdala *et al.* (2016), with the modification that spots were not run in duplicate. Calibration of the instrument was based on the 91500 zircon, which has a $\delta^{18}O$ SMOW (Standard Mean Ocean Water) calibrated value of 9.86 ± 0.11 as based on data from seven gas source mass spectrometry laboratories (Wiedenbeck *et al.* 2004). The total sampling mass for the SIMS oxygen determinations was *ca.* 160 pg as based on white light profilometry.

For trace element composition, the synthetic silicate glass NIST SRM 612 (reference values of Jochum *et al.* 2011) was used as a calibration reference material and stoichiometric Si (SiO_2 = 32.78% *m/m*) as the internal standard element.

Results

Structural study by X-ray powder diffraction and Raman spectroscopy

To evaluate the crystallinity of the samples, unit-cell parameters were obtained by X-ray powder diffraction (Table 2): a_0 varied between 6.6072 ± 0.0005 and 6.6185 ± 0.0004 Å, while c_0 varied between 5.9897 ± 0.0006 and 6.0100 ± 0.0005 Å, which results in a unit-cell volume ranging between 261.481 ± 0.080 and 263.265 ± 0.090 Å^3. The X-ray diffraction (XRD) patterns (Figure 3) are marked by well-defined peaks and low background values. The self-irradiation was quantified from the U and Th mass fractions and the zircon age by calculating the time-integrated alpha dose (D_α) according to the formula (Murakami *et al.* 1991, Nasdala *et al.* 2001):

$$D_\alpha = \frac{6 \cdot c_{Th} \cdot N_A}{10^6 \cdot M_{232}} \cdot (e^{\lambda_{232} t} - 1) + \frac{7 \cdot c_U \cdot 0.0072 \cdot N_A}{10^6 \cdot M_{235}} \cdot (e^{\lambda_{235} t} - 1) + \frac{8 \cdot c_U \cdot 0.9928 \cdot N_A}{10^6 \cdot M_{238}} \cdot (e^{\lambda_{238} t} - 1) \quad (1)$$

where c_U and c_{Th} are the present actinide mass fractions (in μg g^{-1}); N_A is Avogadro's number; M_{238}, M_{235} and M_{232} are the atomic weights of the parent isotopes; λ_{238}, λ_{235} and λ_{232} are the respective decay constants; and t is the integration time in Ma.

The average calculated dose of 0.59 × 10^{18} alpha events per gram corresponds to a 'well-crystallised' structure according to Murakami *et al.* (1991). The unit-cell parameters of BB zircon correspond well to this calculated alpha dose. In addition, the data for BB zircons are within the trend of previously studied, untreated zircon samples from Sri Lanka; however, they are poorer in U and Th (discussed below).

The current degree of radiation damage in the zircons (Figure 4) was determined from the FWHM of the $\nu_3(SiO_4)$ Raman band (internal antisymmetric stretching of SiO_4 tetrahedrons; B1g mode). This band was observed at 1001.6 ± 0.8 cm^{-1}, and its corrected FWHM was determined to be 7.2 ± 0.8 cm^{-1}. These values correspond with mildly to moderately radiation-damaged state of BB zircon,

Table 1.
Summary of the methods employed on twenty BB zircon crystals

Sample	Trace element composition (LA-SF-ICP-MS) – UFOP	Number of analyses												
		ID-TIMS U-Pb dating				LA-Q-ICP-MS U-Pb dating		LA-SF-ICP-MS U-Pb dating		LA-MC-ICP-MS U-Pb dating		LA-MC-ICP-MS Hf isotope analyses		SIMS isotope analyses
		JSGL	NIGL	Oslo	BSU	UFOP	Ports-mouth	UFOP	JWG	UFOP	USP	UFOP	JWG	GFZ
BB1	10	–	–	–	–	–	–	–	8	–	–	–	7	–
BB2	10	–	–	–	–	–	–	–	5	–	–	–	13	–
BB3	10	–	–	–	–	–	–	–	14	–	–	–	20	–
BB4	10	–	–	–	–	–	–	–	6	–	–	–	5	–
BB5	10	–	–	–	–	–	–	–	11	–	–	–	16	–
BB6	10	–	–	–	–	–	–	–	10	–	–	–	5	–
BB7	–	–	–	–	–	–	–	–	–	–	–	–	7	–
BB8	10	–	–	–	–	–	–	–	5	–	–	–	–	–
BB9	10	3	8	3	12	12	30	33	21	9	39	17	3	31
BB10	–	–	–	–	–	–	–	18	–	–	–	13	–	–
BB11	–	–	–	–	–	11	–	20	–	–	–	12	–	–
BB12	16	3	–	3	5	15	–	24	–	24	35	15	–	29
BB13	–	–	–	–	–	14	–	19	–	–	–	12	–	–
BB14	–	–	–	–	–	14	–	20	–	–	–	9	–	–
BB16	–	–	–	–	–	13	–	35	29	–	–	16	–	–
BB17	17	–	–	5	5	13	–	24	–	–	38	11	–	–
BB18	–	–	–	–	–	–	–	–	–	–	–	16	–	–
BB25	35	–	–	–	–	–	–	–	–	–	–	–	–	19
BB39	–	–	–	–	–	–	–	–	–	60	–	–	–	30
BBF	–	–	–	–	–	–	–	–	5	–	–	–	–	–

JSGL – Jack Satterly Geochronology Laboratory (Canada), NIGL – NERC Isotope Geosciences Laboratory (UK), Oslo – University of Oslo (Norway), BSU – Boise State University (USA), UFOP – Federal University of Ouro Preto (Brazil), Portsmouth – University of Portsmouth (UK), JWG – J.W. Goethe University (Frankfurt am Main, Germany), USP – University of Sao Paulo (Brazil), GFZ – Deutsches GeoForschungsZentrum (Potsdam, Germany).

Table 2.
Unit-cell parameters of the BB zircon grains

Analysis	Unit-cell parameters	
	a_0 [Å]	c_0 [Å]
BB9-I	6.6152 ± 0.0006	6.0032 ± 0.0006
BB10	6.6144 ± 0.0003	6.0046 ± 0.0003
BB11	6.6142 ± 0.0003	6.0048 ± 0.0003
BB12-I	6.6147 ± 0.0004	6.0034 ± 0.0004
BB13	6.6185 ± 0.0004	6.0100 ± 0.0005
BB14	6.6144 ± 0.0003	6.0061 ± 0.0004
BB15	6.6072 ± 0.0005	5.9897 ± 0.0006
BB18	6.6141 ± 0.0003	6.0011 ± 0.0003

The α, β and γ angles are 90°.

again corresponding well with the calculated alpha dose for other studied Sri Lankan zircons. Raman work by Nasdala *et al.* (2004) has shown that Sri Lankan zircon retained an average of 55% of the calculated alpha dose per gram. Based on this observation, Nasdala *et al.* (2004) proposed that most studied Sri Lankan zircon should have experienced significant structural recovery through natural annealing.

Trace element and Hf mass fraction

The trace element and Hf mass fractions are presented in Table 3a and b, and also in Figures 5 and 6. Although the individual fragments investigated here are homogeneous on a scale of tens of micrometres, the whole-grain analyses showed a small amount of internal variation, as can be seen in the REE patterns of homogeneous and fractured domains of BB zircons (Figure 6). This variation is observed only in some of the BB grains (e.g., BB17 and BB25) and relates to the CL-bright, fractured domains that returned slightly lower mass fractions in most REEs (Figure 6 and Table 3b) relative to nearby CL-dark domains. Trace element contents also differed slightly between crystals. For example, the average U and radiogenic Pb contents varied between 227 and 368, and 2.1 and 7.9 μg g^{-1}, respectively. The average Th/U ratio varied between 0.20 and 0.47 (based on the values presented in Table 3). Average mass fractions of REEs, such as Ce, Nd, Sm and Eu, varied between 1.3 and 2.3, 0.7 and 3.0, 0.7 and 4.6 and 0.3 and 1.3 μg g^{-1}, respectively. The REEs show steep chondrite-normalised patterns enriched in HREE relative to LREE,

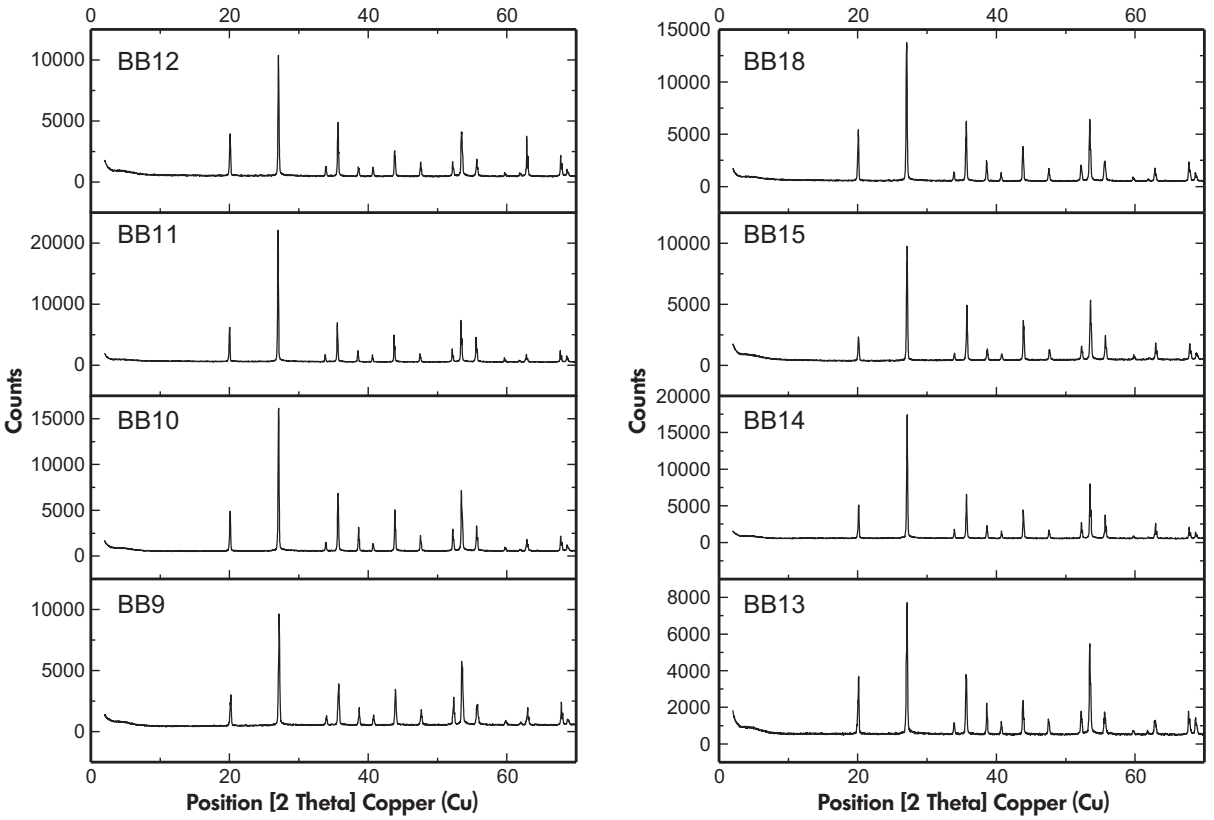

Figure 3. XRD patterns of eight zircon fragments with well-defined peaks and low background values, illustrating the good crystallinity of the BB zircon.

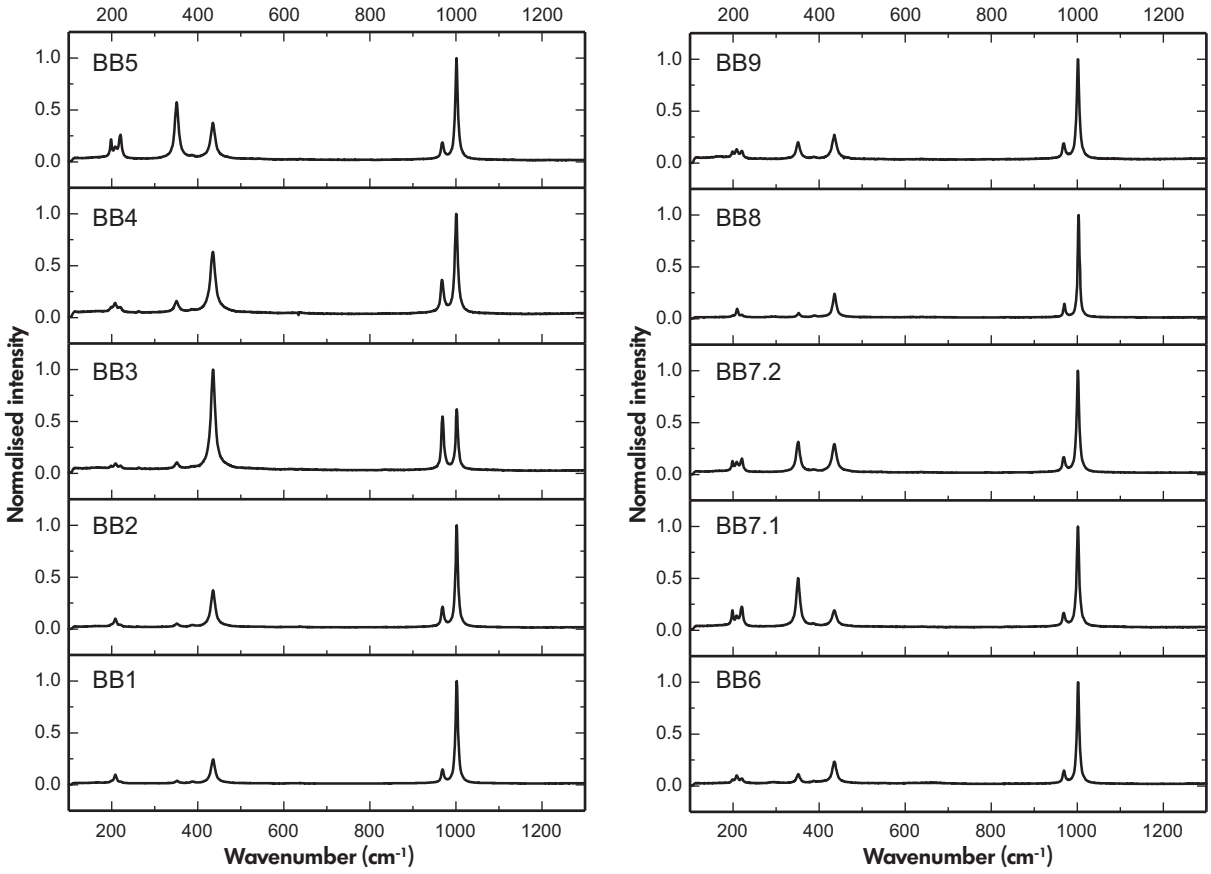

Figure 4. Raman spectra from nine fragments of BB zircon.

small negative Eu and small positive Ce anomaly (La_N/Lu_N varied between 0.0025 and 0.0129, Eu/Eu* varied between 0.53 and 0.73, Ce/Ce* varied between 1.46 and 2.83).

U-Pb dating

Results of ID-TIMS U-Pb dating of different BB crystals are shown in Figure 7 and Appendix S3. The ID-TIMS data have a spread in $^{206}Pb/^{238}U$ and $^{207}Pb/^{206}Pb$ ages from *circa* 565 to 553 Ma and almost all analyses yield $^{206}Pb/^{238}U$ dates that are ~ 0.5% younger than $^{207}Pb/^{206}Pb$ dates, as is found within other high-quality zircon reference materials of Early Palaeozoic to Late Precambrian age (Schoene *et al.* 2006, Mattinson 2010). Each of the crystal fragments yielded approximately the same range of ages, from ~ 554 to ~ 563 Ma for $^{206}Pb/^{238}U$ and ~ 556 to ~ 565 Ma for $^{207}Pb/^{206}Pb$. To investigate the source of scatter in the $^{206}Pb/^{238}U$ and $^{207}Pb/^{206}Pb$ ages, we focus our discussion on the results for crystal BB9 that was analysed in four independent TIMS laboratories (Table 4).

We observed that some of the ages determined by CA-TIMS were similar to those reported by conventional ID-TIMS and that the within-laboratory results from fragments of the same BB9 crystal (e.g., BB9-I, BB9-II, BB9-III, BB9-IV) record a smaller (0.1–0.4%) variation than between different crystal fragments (Figure 7c). The JSGL, NIGL, Oslo fragments yielded similar results within < 1%, while the BSU aliquot gave younger dates within an internal 1% spread of results (Figure 7c). The BSU analyses also show broader scatter (0.4% RSD) than the other laboratories (0.2% RSD; Table 4), suggesting that the BB9-IV aliquot was detectably heterogeneous. Detailed SEM imaging at BSU revealed that some fragments contained dissolution features namely vermiform etch 'tubes', which were created by the chemical abrasion process (Figure 7d, e).

We believe that these vermiform features are likely associated with dislocation tangles created during the long-lived Ratnapura metamorphic event (Kröner *et al.* 1994b, Dissanayake *et al.* 2000, Sajeev *et al.* 2010). The density of such features varies, but they are ubiquitous. Such fractures were preferentially etched during acid washing, suggesting

Table 3a.
Average hafnium and trace element mass fractions of BB zircons

	Mass fractions (μg g^{-1}) ± 1*s* (*n* = 10)							
	BB1[a]	**BB2[a]**	**BB3[a]**	**BB4[a]**	**BB5[a]**	**BB6[a]**	**BB8[a]**	**BB9-I[a]**
Nb	1.07 ± 0.04	2.22 ± 0.09	2.2 ± 0.07	2.1 ± 0.07	2.27 ± 0.06	2.28 ± 0.09	2.25 ± 0.07	2.26 ± 0.08
La	0.28 ± 0.01	0.22 ± 0.02	0.22 ± 0.01	0.21 ± 0.01	0.2 ± 0.02	0.2 ± 0.01	0.21 ± 0.02	0.23 ± 0.02
Ce	2.2 ± 0.09	1.28 ± 0.03	1.91 ± 0.04	2.04 ± 0.06	1.56 ± 0.04	1.82 ± 0.07	1.55 ± 0.08	1.62 ± 0.04
Pr	0.12 ± 0.003	0.1 ± 0.01	0.12 ± 0.01	0.27 ± 0.02	0.13 ± 0.01	0.12 ± 0.01	0.11 ± 0.01	0.12 ± 0.01
Nd	1.3 ± 0.1	0.8 ± 0.1	1.3 ± 0.1	3 ± 0.2	1.3 ± 0.1	1.2 ± 0.1	1 ± 0.1	1 ± 0.1
Sm	1.2 ± 0.3	0.8 ± 0.1	1.2 ± 0.1	4.5 ± 0.1	1.5 ± 0.1	1.1 ± 0.1	0.9 ± 0.1	1 ± 0.1
Eu	0.4 ± 0.04	0.3 ± 0.03	0.4 ± 0.02	1.3 ± 0.05	0.5 ± 0.04	0.4 ± 0.02	0.3 ± 0.02	0.3 ± 0.01
Gd	2.8 ± 0.4	1.9 ± 0.2	2.6 ± 0.3	10.4 ± 0.3	4.1 ± 0.3	2.3 ± 0.1	1.9 ± 0.1	2.1 ± 0.1
Tb	0.7 ± 0.04	0.5 ± 0.02	0.7 ± 0.04	2.6 ± 0.1	1.2 ± 0.04	0.6 ± 0.02	0.5 ± 0.03	0.5 ± 0.02
Dy	6.5 ± 0.3	5.8 ± 0.2	7.7 ± 0.4	27.6 ± 0.5	13.7 ± 0.5	6.8 ± 0.3	6 ± 0.2	5.9 ± 0.1
Ho	2 ± 0.1	1.8 ± 0.1	2.3 ± 0.1	8 ± 0.2	4.3 ± 0.2	2.1 ± 0.1	1.8 ± 0.04	1.8 ± 0.1
Er	8 ± 0.6	8 ± 0.3	10 ± 1	33 ± 0.5	18 ± 0.7	9 ± 0.5	8 ± 0.2	8 ± 0.2
Tm	1.93 ± 0.12	2.02 ± 0.07	2.39 ± 0.13	7.57 ± 0.14	4.35 ± 0.15	2.19 ± 0.09	1.83 ± 0.05	1.83 ± 0.04
Yb	71 ± 1.6	61 ± 1.9	64 ± 2	124 ± 2.6	85 ± 2.4	63 ± 1.6	58 ± 1.1	58 ± 1.7
Lu	2.5 ± 0.2	2.6 ± 0.1	2.9 ± 0.2	8.6 ± 0.1	4.9 ± 0.3	2.7 ± 0.1	2.2 ± 0.1	2.2 ± 0.04
Hf	8403 ± 118	6117 ± 99	5866 ± 71	5960 ± 106	5649 ± 161	6089 ± 105	5983 ± 66	6008 ± 112
Pb	2.1 ± 0.2	3.5 ± 0.1	5.1 ± 0.4	5.7 ± 0.1	3.9 ± 0.2	4.1 ± 0.2	3.4 ± 0.1	3.1 ± 0.1
Th	45 ± 2.1	71 ± 2.2	101 ± 6.7	116 ± 3.3	80 ± 2.6	84 ± 4.1	70 ± 1.2	63 ± 1.5
U	227 ± 13.9	332 ± 6.1	302 ± 8.3	292 ± 5.3	307 ± 9.6	280 ± 9.3	299 ± 4.7	270 ± 3.5
Th/U	0.2 ± 0.01	0.21 ± 0.005	0.33 ± 0.02	0.4 ± 0.01	0.26 ± 0.01	0.3 ± 0.01	0.23 ± 0.01	0.23 ± 0.004
La_N/Lu_N	0.0121 ± 0.0008	0.0089 ± 0.0005	0.008 ± 0.0003	0.0025 ± 0.0001	0.0042 ± 0.0003	0.0078 ± 0.0005	0.01 ± 0.001	0.0109 ± 0.0012
Ce/Ce*	2.78 ± 0.1	2.03 ± 0.13	2.79 ± 0.13	2.04 ± 0.06	2.25 ± 0.11	2.78 ± 0.15	2.36 ± 0.13	2.34 ± 0.12
Eu/Eu*	0.61 ± 0.1	0.73 ± 0.07	0.67 ± 0.04	0.58 ± 0.02	0.61 ± 0.04	0.68 ± 0.05	0.68 ±0.06	0.69 ± 0.04

Table 3b.
Average hafnium and trace element mass fractions in homogeneous/fractured domains

	Mass fractions (μg g^{-1}) ±1*s*					
	BB12[a]		**BB17[a]**		**BB25[a]**	
	Homogeneous	**Fractured**	**Homogeneous**	**Fractured**	**Homogeneous**	**Fractured**
Nb	0.87 ± 0.05	2.25 ± 0.05	1.03 ± 0.04	1.11 ± 0.05	0.83 ± 0.04	1 ± 0.07
La	0.32 ± 0.01	0.24 ± 0.02	0.31 ± 0.02	0.51 ± 0.04	0.21 ± 0.03	0.39 ± 0.03
Ce	1.39 ± 0.16	1.21 ± 0.05	2.77 ± 0.08	2.14 ± 0.08	1.27 ± 0.09	1.36 ± 0.06
Pr	0.15 ± 0.004	0.11 ± 0.01	0.17 ± 0.03	0.22 ± 0.02	0.1 ± 0.01	0.16 ± 0.01
Nd	0.7 ± 0.1	0.8 ± 0.1	2.9 ± 0.1	1.3 ± 0.1	0.8 ± 0.1	0.7 ± 0.1
Sm	0.7 ± 0.02	0.8 ± 0.1	4.6 ± 0.5	1.2 ± 0.2	0.9 ± 0.1	0.6 ± 0.03
Eu	0.3 ± 0.01	0.3 ± 0.02	1.3 ± 0.1	0.4 ± 0.1	0.3 ± 0.04	0.2 ± 0.01
Gd	2.4 ± 0.1	2 ± 0.1	12.5 ± 0.4	3.7 ± 0.9	2.9 ± 0.3	2.3 ± 0.1
Tb	0.5 ± 0.03	0.5 ± 0.02	3.4 ± 0.1	1 ± 0.4	0.9 ± 0.1	0.4 ± 0.04
Dy	5.8 ± 0.2	6.2 ± 0.2	34.7 ± 0.6	11.1 ± 4	10.6 ± 0.7	4.2 ± 0.2
Ho	2 ± 0.1	2 ± 0.1	10.9 ± 0.3	3.6 ± 1.4	3.6 ± 0.2	1.4 ± 0.1
Er	8 ± 0.3	9 ± 0.4	43 ± 1	15 ± 6	15 ± 0.7	6 ± 0.2
Tm	2.11 ± 0.04	2.15 ± 0.1	10.1 ± 0.45	3.75 ± 1.37	3.67 ± 0.18	1.6 ± 0.07
Yb	61 ± 1.1	63 ± 1.6	156 ± 4.6	88 ± 14.5	75 ± 2.2	70 ± 1.5
Lu	2.6 ± 0.1	2.8 ± 0.2	11.5 ± 0.3	4.5 ± 1.6	4.5 ± 0.2	2 ± 0.1
Hf	6160 ± 93	6193 ± 147	8276 ± 166	7895 ± 109	6071 ± 123	8634 ± 197
Pb	3.15 ± 0.15	3.21 ± 0.11	7.92 ± 0.37	4.6 ± 0.33	3.38 ± 0.4	1.92 ± 0.11
Th	77 ± 2.5	68 ± 2.4	174 ± 5.9	104 ± 5.5	73 ± 2.3	43 ± 1.3
U	311 ± 7	312 ± 11.6	368 ± 5.4	341 ± 3.8	296 ± 7.7	211 ± 5.4
Th/U	0.25 ± 0.01	0.22 ± 0.01	0.47 ± 0.01	0.3 ± 0.02	0.25 ± 0.01	0.2 ± 0.005
La_N/Lu_N	0.0129 ± 0.0008	0.0089 ± 0.0005	0.0028 ± 0.0002	0.0133 ± 0.0045	0.0048 ± 0.0006	0.0198 ± 0.0017
Ce/Ce*	1.46 ± 0.15	1.77 ± 0.15	2.83 ± 0.24	1.51 ± 0.13	2.11 ± 0.25	1.27 ± 0.09
Eu/Eu*	0.62 ± 0	0.73 ± 0.04	0.53 ± 0.03	0.54 ± 0.04	0.57 ± 0.06	0.67 ± 0.003
n	9	7	8	9	25	10

[a] LA-SF-ICP-MS data.

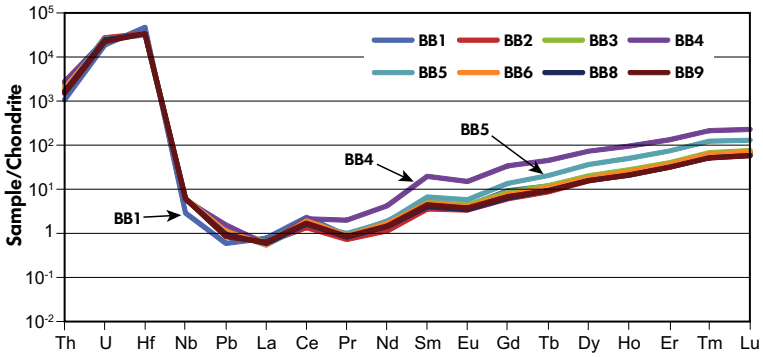

Figure 5. Chondrite-normalised trace element composition of eight fragments of the BB zircon (after Taylor and McLennan 1985).

that they are compositionally distinct in terms of low U and trace element contents, as indicated by the bright zoning of CL images (Figure 2) and trace element analyses (Table 3b).

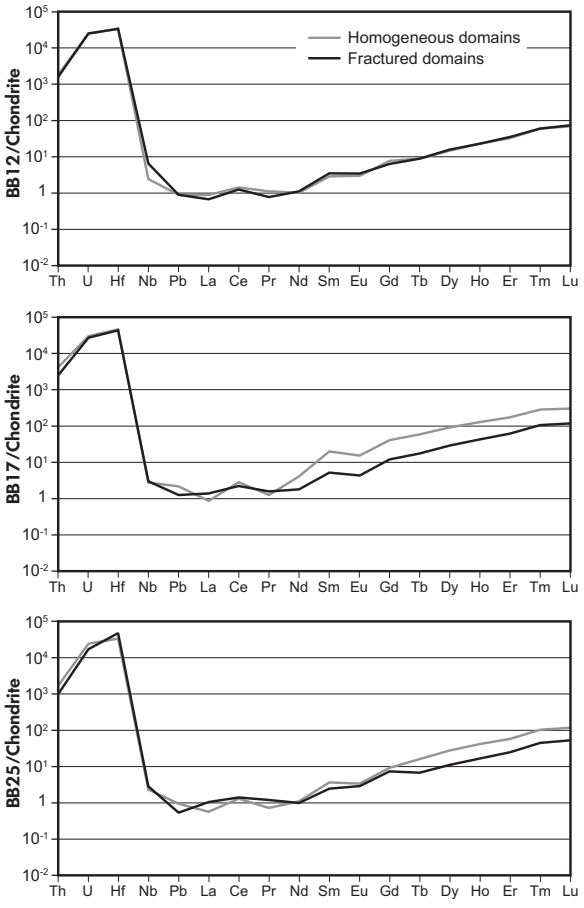

Figure 6. Comparison of the trace element compositions between homogeneous and fractured domains for three individual BB zircons.

The same should apply for grains BB12 and BB17, which show a narrow spread in age for intralaboratory crystal fragments (< 0.4%), but wide age variations (1–1.5%) for results from different laboratories and significantly different parent aliquots of the crystals (Figure 7). The narrow spread in the intralaboratory ages from the same parent aliquots suggests that the grains have highly homogeneous domains, but that careful scrutiny may be required to identify these domains.

Further investigations on the isotopic heterogeneity were made by combining CL imaging and LA-MC-ICP-MS (laser ablation multi-collector-inductively coupled plasma-mass spectrometry) for BB9, BB17 and BB39. To ensure that the results were not affected by instrumental drift, we bracketed the analyses between analyses of two/three other reference materials (Figures 8 and 9). These three BB grains do not universally show strong, patchy CL zoning, but pits and fractures are visible that are interpreted as favourable sites for Pb loss (e.g., Cherniak and Watson 2001; e.g., Figure 2b). Some grains also show oscillatory zoning at their edges. Results of LA-MC-ICP-MS show clear $^{206}Pb/^{238}U$ age variations between dark and bright patchy CL domains. The bright, patchy domains – commonly associated with dissolution pits – yield dates that average at 556 ± 5 Ma (2*s*), 549 ± 7 Ma (2*s*) and 548 ± 7 Ma (2*s*), whereas homogeneous dark domains gave ages that are identical to older TIMS ages obtained for BB9, BB12 and BB17 (average at 561 ± 3 Ma (2*s*) and 562 ± 3 Ma (2*s*)). It is important to note that if CL/BSE and optical imaging are combined, it is possible to separate these domains during analysis.

Spot analyses on BB39 were targeted at fractured domains and oscillatory rims. Surprisingly, the oscillatory rims gave identical dates to those yielded by homogeneous

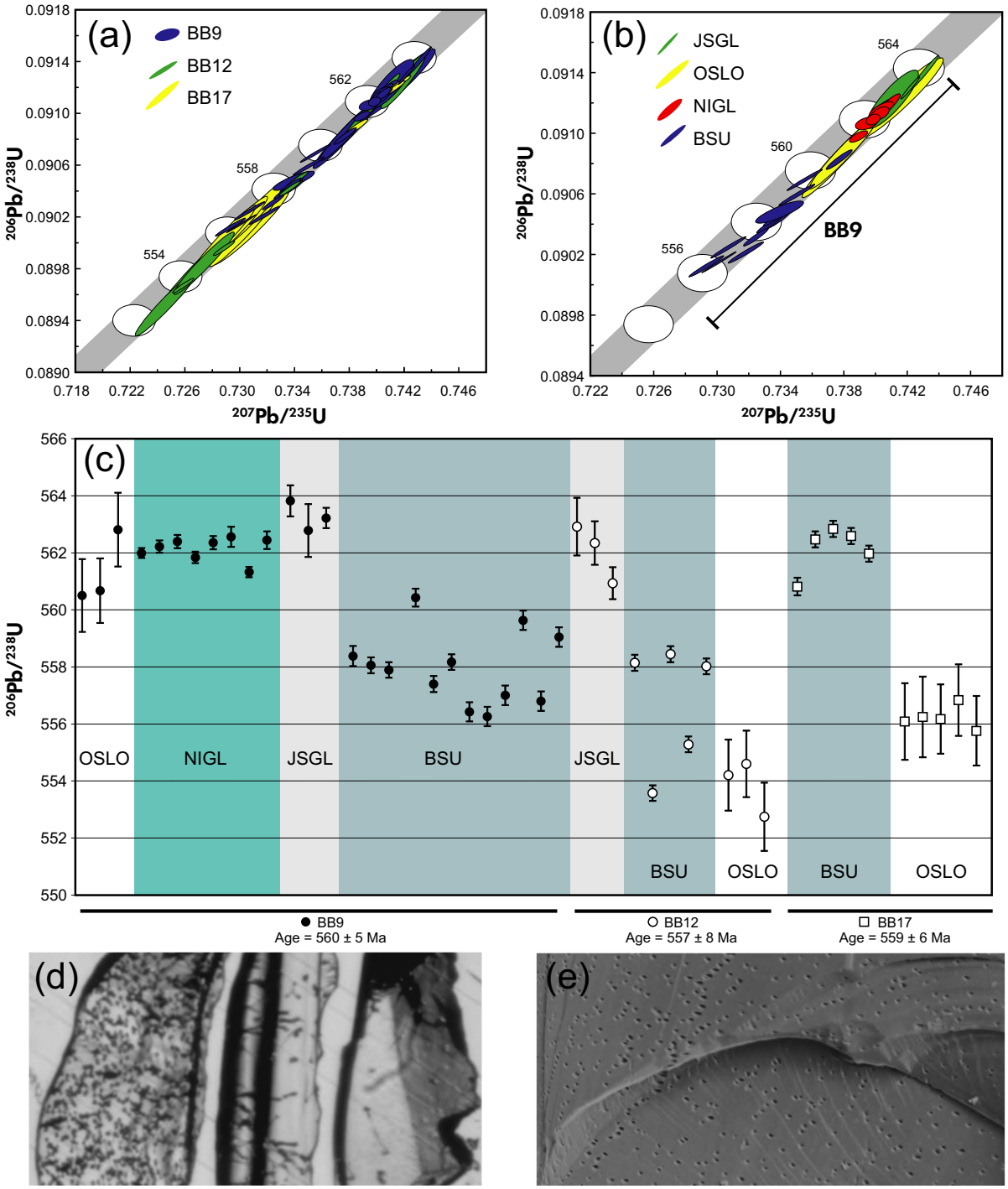

Figure 7. TIMS U-Pb dates of BB zircons: (a) Concordia diagram with all data collected from the Jack Satterly Geochronology Laboratory, NERC Isotope Geosciences Laboratory, University of Oslo and Boise State University. (b) Concordia diagram with all data points for crystal BB9 from the different laboratories. (c) Average $^{206}Pb/^{238}U$ mean dates showing the spread in ages obtained in four TIMS laboratories. (d) Transmitted and (e) BSE images of small fragments of BB showing micrometre-scale dissolution pits and tube-like features.

domains with an average $^{206}Pb/^{238}U$ date of 560 ± 3 Ma (2*s*). Analyses on fractured domains gave a slightly younger $^{206}Pb/^{238}U$ age of 556 ± 4 Ma (2*s*). This shows that each BB megacrysts can produce a number of isotopically homogeneous fragments, suitable for use as either primary calibration or quality control materials. These results also

Table 4.
Summary of ID-TIMS U-Pb and Pb-Pb data for the BB9 zircon

Laboratories	Pb_c (pg)	Atomic ratios							Apparent ages					
		Th/U	$^{206}Pb/^{238}U$	% RSD	$^{207}Pb/^{235}U$	% RSD	$^{207}Pb/^{206}Pb$	% RSD	$^{206}Pb/^{238}U$ (Ma)	% RSD	$^{207}Pb/^{235}U$ (Ma)	% RSD	$^{207}Pb/^{206}Pb$ (Ma)	% RSD
BSU (n = 12) CA-TIMS	0.65	0.24	0.0904 ± 0.0004	0.24	0.7331 ± 0.0048	0.33	0.0588 ± 0.00014	0.12	558 ± 2	0.2	558 ± 2	0.2	560 ± 4	0.4
NIGL (n = 8) CA-TIMS	0.63	0.33	0.0911 ± 0.0002	0.08	0.7401 ± 0.0012	0.09	0.0589 ± 0.00002	0.02	562 ± 0.8	0.1	562 ± 0.8	0.1	564 ± 0.8	0.1
JSGL (n = 3) CA-TIMS	7.95	0.22	0.0913 ± 0.0002	0.1	0.7421 ± 0.0020	0.14	0.0589 ± 0.00006	0.04	563 ± 1	0.1	564 ± 1.2	0.1	565 ± 2	0.2
Oslo (n = 3) ID-TIMS	2.54	0.32	0.0910 ± 0.0004	0.24	0.7391 ± 0.0044	0.29	0.0589 ± 0.00006	0.05	561 ± 2.6	0.2	561 ± 2	0.2	564 ± 2	0.2

Uncertainty estimates are 2s.

show that heterogeneities in the U-Th-Pb system can be detected by careful CL imaging in an analogous manner to the identification and avoidance of domains in other U-Pb reference materials, as in Plešovice zircon, which has U- and Th-rich domains that appear as bright patches on BSE images (Sláma *et al.* 2008).

Interlaboratory comparisons that focused on dating unaltered, CL-dark domains from BB zircons from six different LA-ICP-MS instruments yielded identical results within the limits of the reported analytical uncertainty (Table 5a–c, Figure 10). For instance, the calculated laser ablation ICP-MS ages determined at UFOP, JWG, USP and University of Portsmouth are as follows (for individual analyses, see Appendix S3): by LA-Q-ICP-MS – 563 ± 31 Ma ($^{207}Pb/^{206}Pb$), 562 ± 4 Ma ($^{206}Pb/^{238}U$) and 562 ± 5 Ma ($^{207}Pb/^{235}U$) (2*s*, 92 analyses in seven BB zircons, UFOP, Figure 10a; Table 5a); by LA-SF-ICP-MS – 562 ± 10 Ma ($^{207}Pb/^{206}Pb$), 562 ± 9 Ma ($^{206}Pb/^{238}U$) and 562 ± 7 Ma ($^{207}Pb/^{235}U$) (2*s*, 193 analyses in eight BB zircons, UFOP, Figure 10c; Table 5b); by LA-MC-ICP-MS – 564 ± 7 Ma ($^{207}Pb/^{206}Pb$), 560 ± 6 Ma ($^{206}Pb/^{238}U$) and 561 ± 6 Ma ($^{207}Pb/^{235}U$) (2*s*, 93 analyses in three BB zircons, UFOP, Figure 10e; Table 5c); by LA-SF-ICP-MS - 561 ± 9 Ma ($^{207}Pb/^{206}Pb$), 562 ± 6 Ma ($^{206}Pb/^{238}U$) and 562 ± 5 Ma ($^{207}Pb/^{235}U$) (2*s*, 114 analyses in ten BB zircons, JWG, Figure 10d; Table 5b); by LA-MC-ICP-MS - 570 ± 61 Ma ($^{207}Pb/^{206}Pb$), 562 ± 9 Ma ($^{206}Pb/^{238}U$) and 564 ± 16 Ma ($^{207}Pb/^{235}U$) (2*s*, 112 analyses in three BB zircons, USP, Figure 10f; Table 5c); and by LA-Q-ICP-MS - 567 ± 44 Ma ($^{207}Pb/^{206}Pb$), 562 ± 22 Ma ($^{206}Pb/^{238}U$) and 558 ± 16 Ma ($^{207}Pb/^{235}U$) (2*s*, 30 analyses in one BB zircon, University of Portsmouth, Figure 10b; Table 5a).

Thus, we conclude that fragments of BB crystals marked by CL dark and which are weakly zoned in BSE imaging are isotopically homogeneous and record identical ages at the level of precision documented by hundreds of laser ablation analyses (e.g., Figure 10). Because the BB grains are large (> 1 cm), domains within the megacrystals may record younger ages, which in the cases of BB9, BB12 and BB17 resulted in a 9–10 Ma spread in ID-TIMS dates. Nevertheless, these domains can be easily avoided using detailed CL imaging and some LA-MC-ICP-MS U-Pb dating prior to distribution.

Judging from the great number of ID-TIMS analyses obtained here, the BB zircon group is considered one of the best characterised reference material for LA-ICP-MS geochronology (Table 6a), in the sheer number of discrete analyses across laboratories that have been undertaken. The BB suite is also one of the most abundant materials for

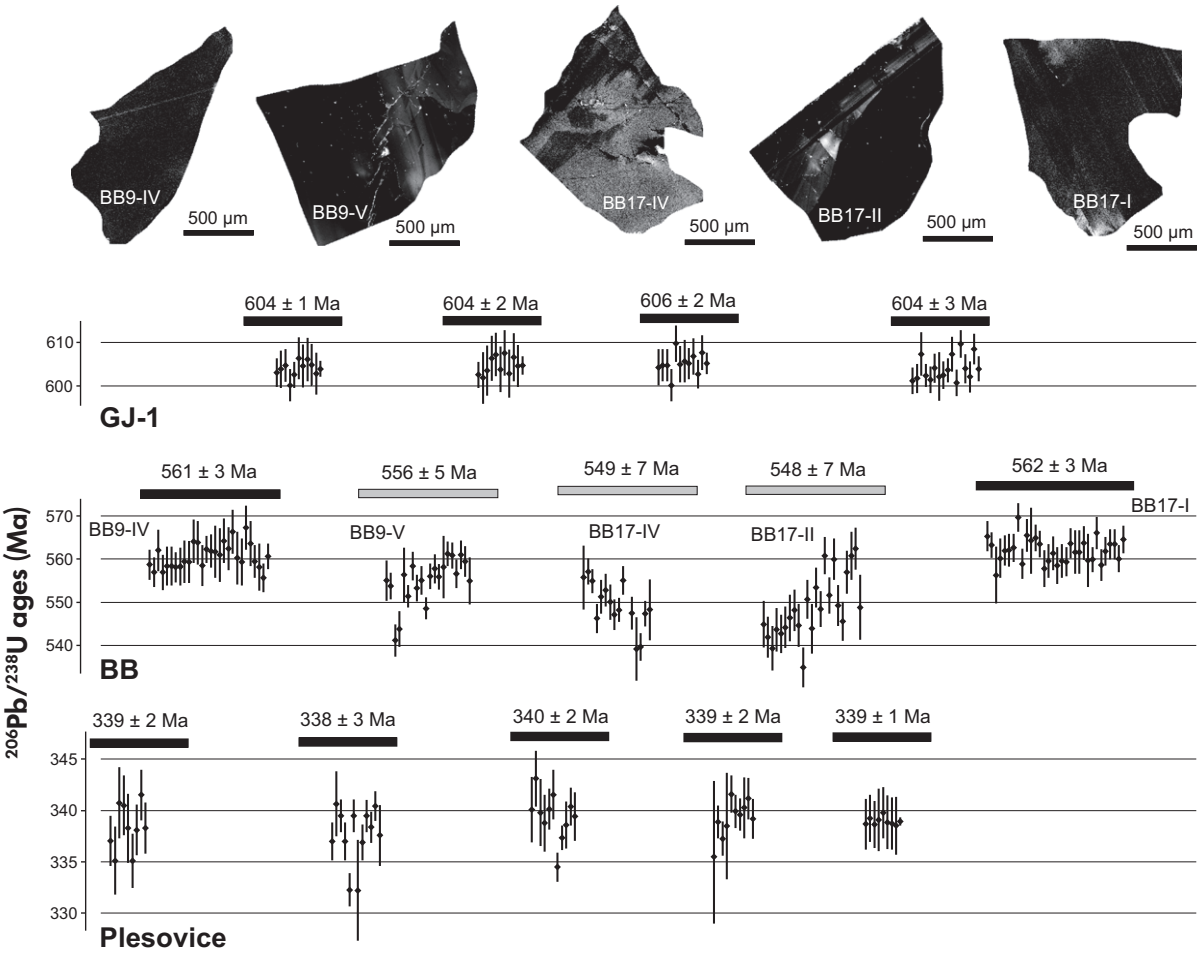

Figure 8. Cathodoluminescence images (top) of fragments, showing some patchy domains, and LA-MC-ICP-MS U-Pb dates (obtained at UFOP) of BB, GJ-1 and Plešovice zircon reference materials. Grey bars for BB fragments correspond to bright, patchy domains in fragments BB9-V, BB17-IV and BB17-II, whereas black bars are for BB9-IV and BB17-I. Error bars are 2*s*.

distributing to LA-ICP-MS laboratories. BB grains show similar U and Pb mass fractions to those reported for the GJ-1 and Plešovice reference materials, and it has substantially greater Hf mass fractions than other reference materials (Table 6a). All analysed fragments showed low levels of common Pb and high U and radiogenic Pb mass fractions, yielding high count rates and good counting statistics. If all TIMS ages are considered, the BB12, BB9 and BB17 show a 1–2% (10 My) spread in $^{206}Pb/^{238}U$ ages (forty-seven TIMS analyses) that is slightly larger (within a ± 1 Ma uncertainty of apparent ages) than that published for GJ-1 (7 Ma – based on eight ID-TIMS analyses; Jackson *et al.* 2004) and for 91500 (7 Ma – eleven ID-TIMS analyses; Wiedenbeck *et al.* 1995). However, the spread in ages can be reduced (< 0.8% – 4 Ma) if the dates for the individual domain types are considered. Table 6b shows averaged results of TIMS values recommend for the homogeneous domains after CL imaging of individual fragments. We advise that, if constraints better than 1% are required for the use of the material, the distributed fragments should be analysed by ID-TIMS for better constraints on uncertainty propagation. It is important to note that different geological analyses require different levels of precision, in other words, in the case of analyses that do not require the highest level of accuracy (e.g., detrital zircon studies), BB zircon can be completely suitable as characterised in this work. However, if further information is required, then, ID-TIMS might be needed.

The performance of the BB9 zircon as a primary reference material for laser ablation ICP-MS analysis was assessed via laser ablation SF-ICP-MS measurements of four other zircon reference materials, namely Plešovice, M127 (Nasdala *et al.* 2016), GJ-1 and 91500. The analyses were calibrated against the BB9 crystal. Table 7 shows data obtained for the other zircon reference materials, using BB9 as primary calibrant and assuming 562 Ma ($^{207}Pb/^{206}Pb$),

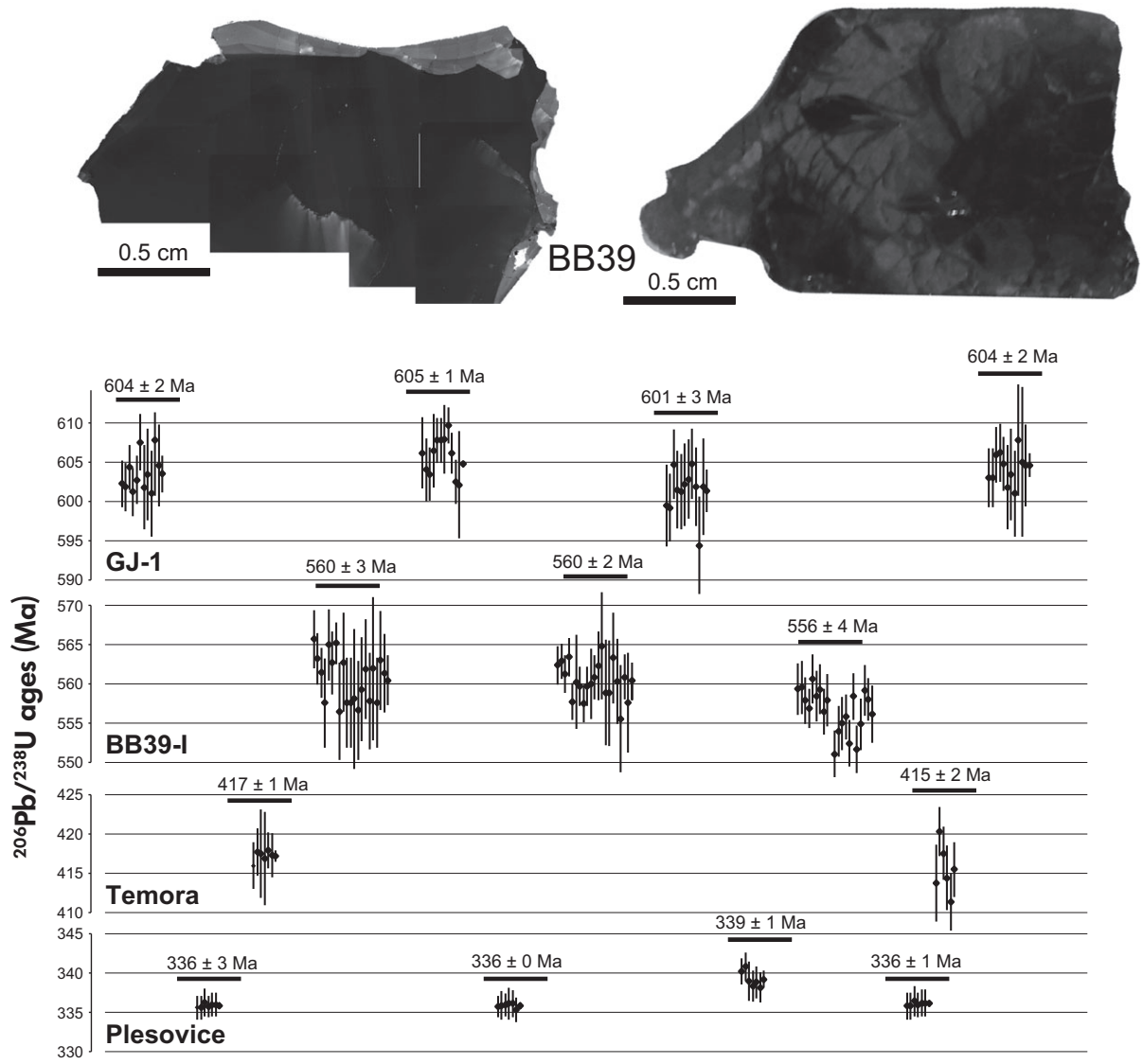

Figure 9. Whole-grain imaging via cathodoluminescence (top left) and transmitted light (top right), and LA-MC-ICP-MS U-Pb dates (obtained at the Federal University of Ouro Preto) for BB39, GJ-1, Temora and Plešovice zircon reference materials. Uncertainty estimates are 2*s*.

560 Ma ($^{206}Pb/^{238}U$) and 561 Ma ($^{207}Pb/^{235}U$) (mean of TIMS ages; Table 4). The analyses of these reference materials using BB9 as calibrant in each case returned Concordia ages that were well within analytical uncertainty of the accepted age of the reference materials (Table 7). Problems in the analysis of the other zircon reference materials (as for instance irregular sputtering behaviour, high ^{204}Pb count rates, U-Pb discordance) were not observed. Therefore, there appear to be no performance problems that would preclude the use of the BB9 zircon as a primary calibrant for laser ablation ICP-MS. In addition, at the University of Portsmouth, a small amount of data was collected using BB9 as a primary reference material. In this arrangement, 91500 yielded $^{206}Pb/^{238}U$ and $^{207}Pb/^{206}Pb$ ages of 1065 ± 59 and 1063 ± 56 Ma (n = 3, 2*s*), respectively, that are consistent with published values.

Hf isotope composition

The Hf mass fraction of the different BB zircon grains was found to vary between 0.56 and 0.84 g/100 g (Table 3). Laser ablation MC-ICP-MS data suggest a homogeneous Hf isotope composition (Figure 11) both within and between individual zircon grains. A mean of Lu/Hf of 0.00008 and of $^{176}Hf/^{177}Hf$ for the pooled data set of 0.281674 ± 0.000018 (2*s*, 197 analyses from sixteen grains) were

Table 5a.
Summary of laser ablation Q-ICP-MS U-Pb data for BB zircon fragments.

Analysis	Atomic ratios						Apparent ages (Ma)					
	$^{207}Pb/^{235}U$	2*s* (abs)	$^{206}Pb/^{238}U$	2*s* (abs)	$^{207}Pb/^{206}Pb$	2*s* (abs)	$^{207}Pb/^{235}U$	2*s* (abs)	$^{206}Pb/^{238}U$	2*s* (abs)	$^{207}Pb/^{206}Pb$	2*s* (abs)
UFOP BB9 (*n* = 12)	0.7415	0.0099	0.0912	0.0008	0.0590	0.0010	563	6	562	5	568	37
UFOP BB11 (*n* = 11)	0.7382	0.0099	0.0909	0.0009	0.0589	0.0010	561	6	561	5	565	37
UFOP BB12 (*n* = 15)	0.7395	0.0083	0.0911	0.0006	0.0589	0.0007	562	5	562	3	564	26
UFOP BB13 (*n* = 14)	0.7401	0.0056	0.0911	0.0009	0.0589	0.0006	562	4	562	5	565	23
UFOP BB14 (*n* = 14)	0.7402	0.0095	0.0911	0.0007	0.0590	0.0009	562	6	562	4	565	32
UFOP BB16 (*n* = 13)	0.7368	0.0130	0.0911	0.0005	0.0587	0.0010	561	8	562	3	556	38
UFOP BB17 (*n* = 13)	0.7380	0.0069	0.0910	0.0009	0.0588	0.0007	561	4	562	5	560	25
UFOP ALL (*n* = 92)	0.7392	0.0090	0.0911	0.0008	0.0589	0.0008	562	5	562	4	563	31
Portsmouth BB9 (*n* = 30)	0.7334	0.0269	0.0911	0.0037	0.0590	0.0012	558	16	562	22	567	44

Table 5b.
Summary of laser ablation SF-ICP-MS U-Pb data for BB zircons

Summary	Atomic ratios						Apparent ages (Ma)					
	$^{207}Pb/^{235}U$	2*s*	$^{206}Pb/^{238}U$	2*s*	$^{207}Pb/^{206}Pb$	2*s*	$^{207}Pb/^{235}U$	2*s*	$^{206}Pb/^{238}U$	2*s*	$^{207}Pb/^{206}Pb$	2*s*
JWG BB1 (*n* = 8)	0.7392	0.0059	0.0912	0.0005	0.0588	0.0002	562	3	563	4	560	4
JWG BB2 (*n* = 5)	0.7411	0.0078	0.0913	0.0009	0.0589	0.0002	563	4	563	5	564	5
JWG BB3 (*n* = 14)	0.7389	0.0088	0.0911	0.0010	0.0588	0.0002	562	5	562	6	560	4
JWG BB4 (*n* = 6)	0.7408	0.0097	0.0913	0.0010	0.0588	0.0002	563	6	563	6	561	5
JWG BB5 (*n* = 11)	0.7378	0.0132	0.0910	0.0014	0.0588	0.0002	561	8	562	8	559	7
JWG BB6 (*n* = 10)	0.7391	0.0068	0.0912	0.0007	0.0588	0.0001	562	4	563	4	559	4
JWG BB8 (*n* = 5)	0.7369	0.0064	0.0910	0.0007	0.0588	0.0001	561	4	561	4	558	5
JWG BB9. (*n* = 21)	0.7426	0.0147	0.0913	0.0010	0.0590	0.0008	564	9	563	6	568	29
JWG BB16 (*n* = 29)	0.7394	0.0142	0.0910	0.0016	0.0589	0.0006	562	8	562	10	564	23
JWG BBF (*n* = 5)	0.7376	0.0066	0.0910	0.0007	0.0588	0.0001	561	4	561	4	559	4
JWG ALL (114)	0.7393	0.0094	0.0911	0.0010	0.0588	0.0003	562	5	562	6	561	9
UFOP BB9 (*n* = 33)	0.7379	0.0129	0.0909	0.0014	0.0589	0.0004	561	7	561	8	562	11
UFOP BB10 (*n* = 18)	0.7416	0.0100	0.0913	0.0011	0.0589	0.0002	563	8	563	9	565	11
UFOP BB11 (*n* = 20)	0.7373	0.0136	0.0908	0.0018	0.0589	0.0002	561	8	560	11	563	9
UFOP BB12 (*n* = 24)	0.7383	0.0109	0.0909	0.0014	0.0589	0.0004	561	6	561	8	563	14
UFOP BB13 (*n* = 19)	0.7401	0.0095	0.0911	0.0013	0.0589	0.0004	562	6	562	8	566	14
UFOP BB14 (*n* = 20)	0.7365	0.0127	0.0913	0.0016	0.0585	0.0001	561	8	563	10	550	4
UFOP BB16 (*n* = 35)	0.7410	0.0118	0.0912	0.0014	0.0589	0.0003	563	7	563	8	564	9
UFOP BB17 (*n* = 24)	0.7423	0.0106	0.0914	0.0012	0.0589	0.0001	564	6	564	7	565	5
UFOP ALL (193)	0.7394	0.0115	0.0911	0.0014	0.0589	0.0003	562	7	562	9	562	10

Table 5c.
Summary of laser ablation MC-ICP-MS U-Pb data for BB zircons

Summary	Atomic ratios						Apparent ages (Ma)					
	$^{207}Pb/^{235}U$	2*s*	$^{206}Pb/^{238}U$	2*s*	$^{207}Pb/^{206}Pb$	2*s*	$^{207}Pb/^{235}U$	2*s*	$^{206}Pb/^{238}U$	2*s*	$^{207}Pb/^{206}Pb$	2*s*
UFOP BB9-I (n = 9)	0.7378	0.0116	0.0908	0.0011	0.0590	0.0002	561	7	560	7	566	7
UFOP BB12-I (n = 24)	0.7376	0.0084	0.0908	0.0009	0.0589	0.0002	561	5	560	5	564	7
UFOP BB39.1 (n = 60)	0.7349	0.0124	0.0906	0.0012	0.0588	0.0002	559	7	559	7	561	8
UFOP ALL (n = 93)	0.7368	0.0108	0.0907	0.0011	0.0589	0.0002	561	6	560	6	564	7
USP BB9 (n = 39)	0.7420	0.0237	0.0910	0.0016	0.0592	0.0014	564	14	561	9	573	54
USP BB12 (n = 35)	0.7479	0.0277	0.0914	0.0016	0.0594	0.0017	567	16	564	10	581	62
USP BB17 (n = 38)	0.7377	0.0299	0.0911	0.0014	0.0588	0.0018	561	17	562	8	558	69
USP ALL (n = 112)	0.7425	0.0271	0.0911	0.0016	0.0591	0.0017	564	16	562	9	570	61

For key to measurement laboratories see footnote to Table 1 and main text. Table 5 individual analyses are reported in online supporting information.

measured. For reference zircons, $^{176}Hf/^{177}Hf$ values of 0.28167 ± 0.00002 (2*s*) and $^{178}Hf/^{177}Hf$ values of 1.46720 ± 0.00004 (2*s*) were obtained on JWG and $^{176}Hf/^{177}Hf$ values of 0.28168 ± 0.00001 (2*s*) and $^{178}Hf/^{177}Hf$ values of 1.46726 ± 0.00001 (2*s*) were obtained on UFOP (Table 8 – for individual analyses, see Appendix S4), and with a mean $^{176}Hf/^{177}Hf$ for the pooled data set of 0.281674 ± 0.000018 (2*s*, 197 analyses from sixteen grains).

The laser ablation Hf isotope data obtained from the two laboratories are identical within analytical uncertainty, showing only a negligible difference in the results obtained for JWG and UFOP. The Hf isotope composition of the studied zircons measured at the JWG shows somewhat large variation of the $^{176}Hf/^{177}Hf$ ratios within, and between, individual grains (*cf.* Figure 11). This might suggest some minor inter- and intragrain heterogeneity of the Hf isotope composition may have been detected at JWG. However, we suspect that the reported variations relate to the amount of material sampled during laser ablation, given that the laser conditions (spot size and energy) were different between the two laboratories. For instance, at JWG spot sizes were substantially smaller (40 μm spots) than at UFOP (50 μm spots). This difference translated into much smaller uncertainty estimates for single measurements at UFOP, whereas the mean values remained essentially the same.

The BB zircon grains have an average ε_{Hf} (at 561 Ma) for the pooled data set of -26.9 ± 0.6 (2*s*, Figure 11). All grains were marked by low Lu/Hf (averages of 0.00006 and 0.00009) and Yb/Hf (averages of 0.000004 and 0.000005) ratios. Further assessment of the suitability of BB zircons as a reference material for Hf isotope determination will require solution MC-ICP-MS data, which are beyond the scope of this contribution.

Oxygen isotope systematics

SIMS results of this study are reported in Table 9, and a photograph of the sample mount is provided in Appendix S2. Twenty-seven interspersed analyses of the 91500 zircon from a single millimetre-sized area showed no significant drift in the $^{18}O^-/^{16}O^-$ ratio over a period of 17 h. Hence, no drift correction was necessary. Another group of n = 30 determinations on a total of three chips from 91500 yielded a value for the total fractionation of 1.0022268 ± 0.24‰ (2*s*); this value being based on the assigned $\delta^{18}O$ SMOW composition for 91500 of 9.98‰ (Wiedenbeck *et al.* 2004). This value for instrumental bias was applied to all other oxygen isotope ratio results obtained during this study. The three quality control materials Penglai (Li *et al.* 2010), Plešovice and Temora 2 (Black *et al.*

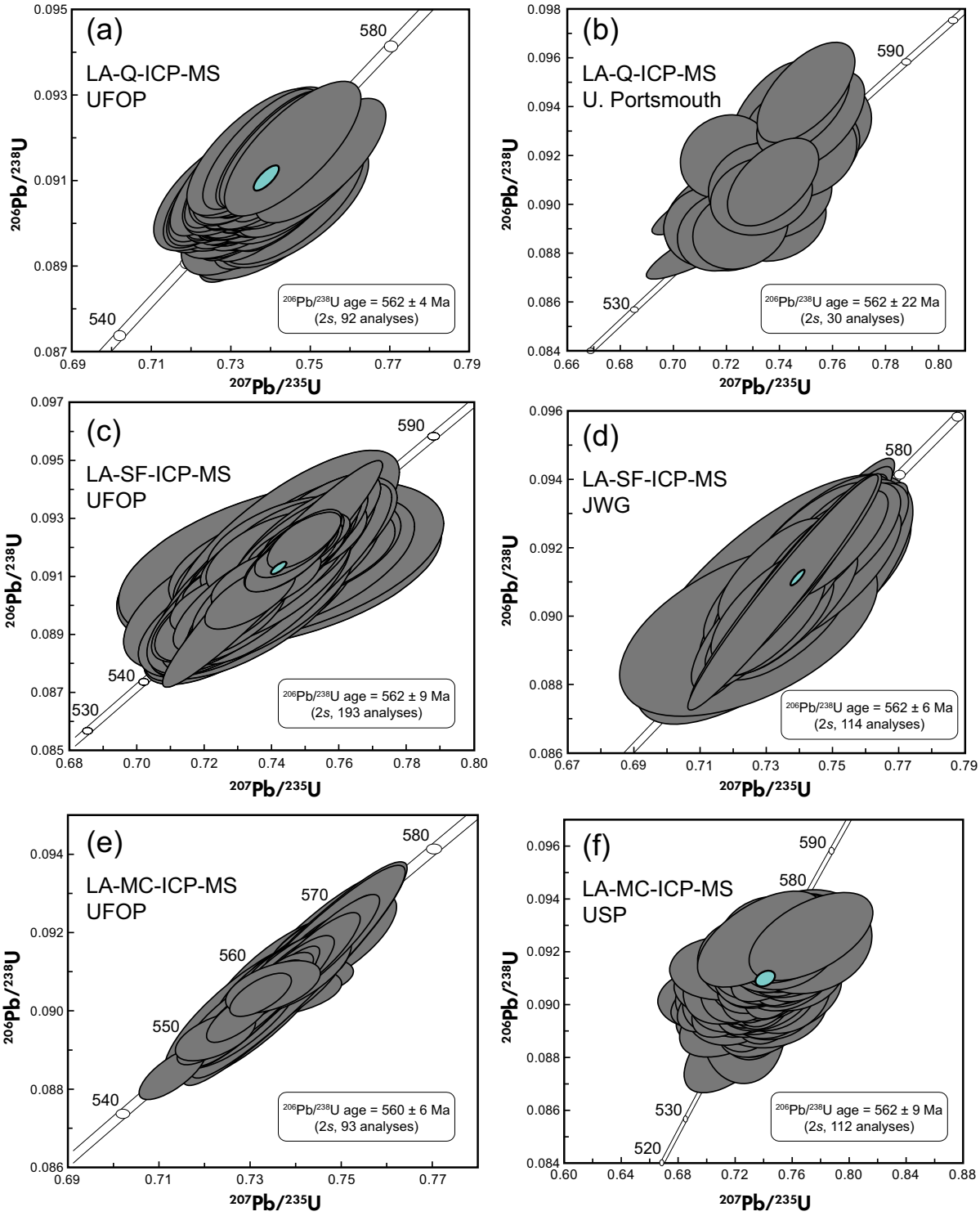

Figure 10. Laser ablation ICP-MS U-Pb ages obtained using: (a) Q-ICP-MS – Federal University of Ouro Preto (UFOP), (b) Q-ICP-MS – University of Portsmouth, (c) SF-ICP-MS – UFOP, (d) SF-ICP-MS – J.W. Goethe University of Frankfurt am Main, (e) MC-ICP-MS – UFOP and (f) MC-ICP-MS – University of São Paulo.

2004) all gave results that were within 0.4‰ of their published values, so we conclude that our data are reliable with an overall uncertainty of better than ± 1‰ (2*s*). The source of the systematic offset between 91500 and the other reference materials remains unclear, and this pattern has been seen in other, as yet unpublished, data sets from the

Table 6a.
Summary of zircon reference material data

Refer ence material	Number of ID-TIMS analyses	Number of ID-TIMS laboratories	Number of crystals analysed by ID-TIMS	$^{206}Pb/^{238}U$ ID-TIMS age (Ma)	U (μg g^{-1})	Pb_{rad} (μg g^{-1})	Hf (μg g^{-1})	Grain size	Reference
91500	11	3	1	1059.2–1065.5	71–86	13–16	5610–29748	238 g	Wiedenbeck *et al.* (1995), Griffin *et al.* (2006)
GJ-1	8	1	4	596.2–602.7	212–422	19.3–37.4	~ 6558	*ca.* 1 cm	Jackson *et al.* (2004), Morel *et al.* (2008)
M257	34	4	1	559.3–564.1	812–863	52.0–90.1		19.5 mm	Nasdala *et al.* (2008)
Temora	21	1	3	415.25–417.82	60–600	~ 14.3	~ 8310	0.05–0.3 mm	Black *et al.* (2003, 2004)
Plešovice	27	5	7	336.15–337.70	465–3084	21–158	8980–14431	1–6 mm	Sláma *et al.* (2008)
BB BB9	47	26	4	556–564	263–275	2.9–3.4	5793–6129		
BB BB12		11	3	553–563	227–368 302–321	2.1–7.9 2.9–3.4	5649– 5979–6321	Up to 1 cm;	This work
BB BB17		10	2	556–563	361–378	7.5–8.6	8403 8052–8592	~300 g	

Table 6b.
Recommended values for the BB zircon reference materials

Sample	Pb_c (pg)[a]	Atomic ratios									Apparent ages (Ma)					
		Th/U[b]	$^{206}Pb/^{204}Pb$[c]	$^{207}Pb/^{235}U$[d]	± (%)[e]	$^{206}Pb/^{238}U$[d]	± (%)[e]	$^{207}Pb/^{206}Pb$[d]	± (%)[e]	$^{207}Pb/^{235}U$[f]	±[g]	$^{206}Pb/^{238}U$[f]	±[g]	$^{207}Pb/^{206}Pb$[f]	±[g]
BB9 (n = 26)	1.70	0.27	75613.27	0.736983	0.000868	0.090797	0.000073	0.058867	0.000032	561	0.5	560	0.4	562	1.2
BB12 (*n* = 11)	1.99	0.30	112764.82	0.732341	0.001073	0.090313	0.000113	0.058767	0.000030	558	0.6	557	0.7	560	1.0
BB17 (*n* = 10)	2.45	0.22	122288.40	0.735291	0.001329	0.090616	0.000134	0.058850	0.000034	560	0.8	559	0.8	562	1.3

[a] Total mass of common Pb. [b] Th contents calculated from radiogenic ^{208}Pb and the $^{207}Pb/^{206}Pb$ date of the sample, assuming concordance between U-Th and Pb systems. [c]Measured ratio corrected for fractionation and spike contribution only. [d] Corrected for fractionation, spike and blank. All common Pb was assumed to be procedural blank. $^{206}Pb/^{238}U$ ratio corrected for initial disequilibrium in $^{230}Th/^{238}U$ using Th/U [magma] = 4 ± 1. [e] Uncertainties are 2*s*, propagated using the algorithms of Schmitz and Schoene (2007) and Crowley *et al.* (2007). [f] Calculations are based on the decay constants of Jaffey *et al.* (1971). $^{206}Pb/^{238}U$ date corrected for initial disequilibrium in $^{230}Th/^{238}U$ using Th/U [magma] = 4 ± 1. [g] Errors are 2*s*.

Table 7.
Results of laser ablation SF-ICP-MS U-Pb analyses of other zircon reference materials when calibrated *versus* BB zircon

Sample	Published age (Ma)	*n*	Determined age[a] when calibrated *versus* BB9 zircon		
			$^{207}Pb/^{235}U$	$^{206}Pb/^{238}U$	$^{207}Pb/^{206}Pb$
Plešovice	337	17	337 ± 1	337 ± 1	341 ± 13
M127	524	16	524 ± 3	524 ± 3	525 ± 12
GJ1	608	19	609 ± 2	607 ± 2	618 ± 13
91500	1065	12	1072 ± 7	1066 ± 5	1084 ± 23

[a] Calculated ages are weighted mean values. Uncertainties are quoted at the 95% confidence level; they include the uncertainty of the reference analyses.

Potsdam laboratory. We suspect this effect might be related to the lack of a well-established traceability chain between the assigned values for the various materials.

The four BB zircon crystals studied during the oxygen part of this project all produced similar $\delta^{18}O$ SMOW values, with an overall mean of 13.16 ± 0.78‰ (*n* = 109, 2*s*); this result is similar to the value of $\delta^{18}O$ = 13.9 for the M257 Sri Lankan gem reference material reported by Nasdala *et al.* (2008), but contrast with the value of $\delta^{18}O$ = 8.3 reported for M127 reference materials (Nasdala *et al.* 2016), which is also of Sri Lankan origin (Figure 12). The overall $\delta^{18}O$ reproducibility on the four BB samples of only ± 0.78‰ (2*s*) indicates that real oxygen isotope ratio variations exist within the BB sample suite. A closer look reveals that the BB9 and BB12 crystals are some 0.5‰ heavier in their oxygen isotope compositions than is the case for the BB25 and BB39 crystals. Of the four grains that were studied for oxygen isotope systematics, the BB39 crystal shows the best reproducibility at ± 0.20‰ (2*s*, *n* = 30 determinations on *n* = 3 fragments, 2*s*). This is as good as the reproducibility determined for both the 91500 primary calibrant as well as the Penglai and Plešovice quality control materials, and hence, we conclude from our data set there is no evidence for oxygen isotope heterogeneity in the BB39 crystal. The overall range for the entire suite of BB material investigated here is small (± 0.78‰ at 2*s* level), suggesting that the material may be cogenetic in its origin.

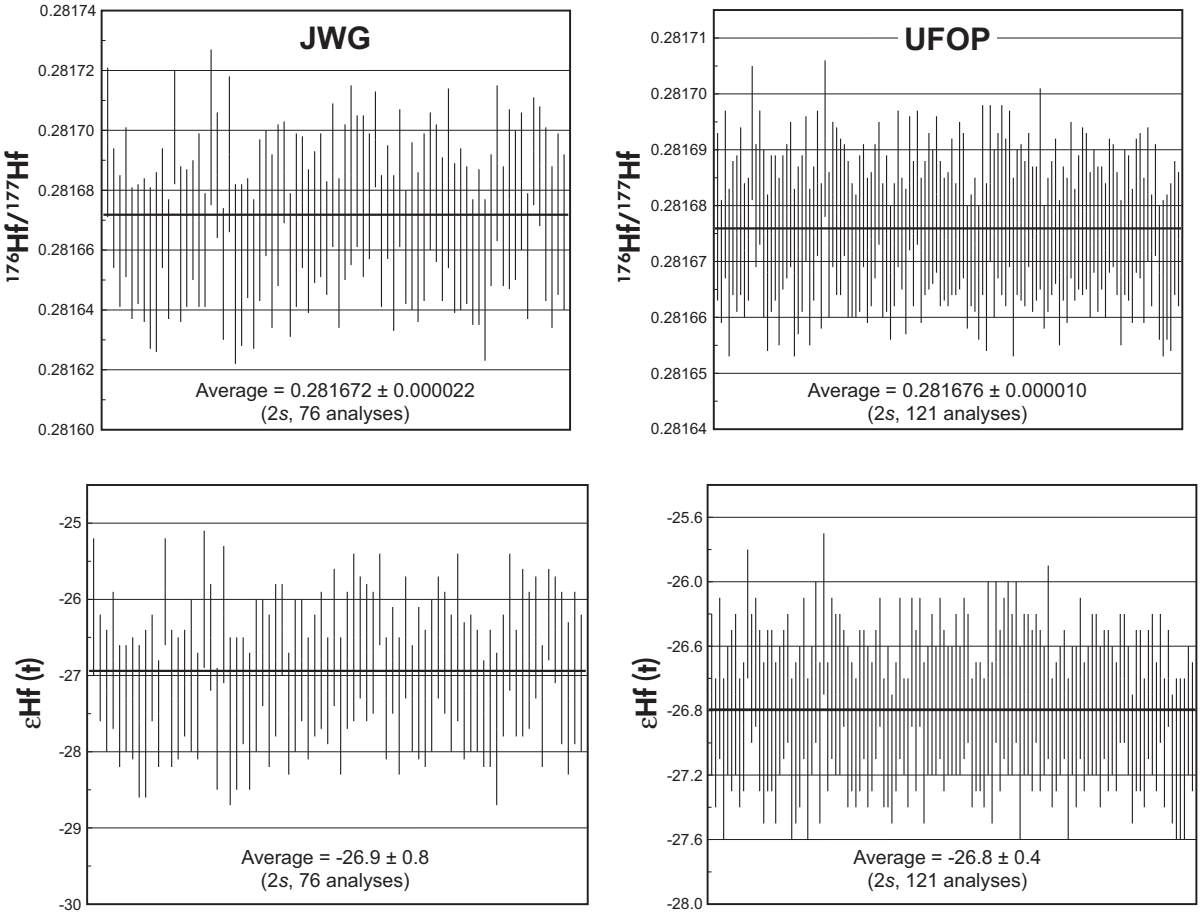

Figure 11. Hf isotope composition of the BB zircon samples obtained by laser ablation MC-ICP-MS analyses.

Table 8.
Summary of laser ablation MC-ICP-MS measurements of Hf isotope composition in the BB zircon

Analysis	Lu/Hf	Yb/Hf	$^{176}Hf/^{177}Hf$	2*s*	$^{178}Hf/^{177}Hf$	$^{180}Hf/^{177}Hf$	εHf_{561}	2*s*
JWG BB1 (*n* = 7)	0.00003	0.000002	0.281670	0.000027	1.46719	1.88663	-27.0	0.9
JWG BB2 (*n* = 13)	0.00015	0.000009	0.281670	0.000033	1.46720	1.88675	-27.1	1.2
JWG BB3 (*n* = 20)	0.00006	0.000004	0.281669	0.000023	1.46719	1.88676	-27.0	0.8
JWG BB4 (*n* = 5)	0.00005	0.000003	0.281684	0.000016	1.46721	1.88663	-26.5	0.6
JWG BB5 (*n* = 16)	0.00006	0.000004	0.281669	0.000018	1.46719	1.88682	-27.0	0.7
JWG BB6 (*n* = 5)	0.00004	0.000002	0.281668	0.000029	1.46723	1.88683	-27.1	1.0
JWG BB7 (*n* = 7)	0.00004	0.000002	0.281678	0.000023	1.46718	1.88676	-26.7	0.8
JWG BB9 (*n* = 3)	0.00005	0.000003	0.281666	0.000011	1.46723	1.88683	-27.1	0.4
JWG BB ALL	0.00006	0.000004	0.281672	0.000022	1.46720	1.88675	-26.9	0.8
UFOP BB9 (*n* = 17)	0.00008	0.000005	0.281676	0.000013	1.46726	1.88687	-26.8	0.4
UFOP BB10 (*n* = 13)	0.00016	0.000010	0.281677	0.000014	1.46725	1.88669	-26.8	0.5
UFOP BB11 (*n* = 12)	0.00010	0.000006	0.281676	0.000008	1.46726	1.88679	-26.8	0.3
UFOP BB12 (*n* = 15)	0.00015	0.000009	0.281677	0.000011	1.46725	1.88679	-26.8	0.4
UFOP BB13 (*n* = 12)	0.00004	0.000003	0.281675	0.000009	1.46726	1.88680	-26.8	0.3
UFOP BB14 (*n* = 9)	0.00005	0.000003	0.281678	0.000010	1.46727	1.88670	-26.7	0.4
UFOP BB16 (*n* = 16)	0.00005	0.000003	0.281676	0.000009	1.46726	1.88679	-26.8	0.3
UFOP BB17 (*n* = 11)	0.00005	0.000003	0.281677	0.000006	1.46725	1.88680	-26.8	0.2
UFOP BB18 (*n* = 16)	0.00012	0.000007	0.281675	0.000010	1.46725	1.88678	-26.9	0.4
UFOP BB ALL	0.00009	0.000005	0.281676	0.000010	1.46726	1.88678	-26.8	0.4

JWG, J.W. Goethe University of Frankfurt am Main; UFOP, Federal University of Ouro Preto. εHf_{561} calculated as an initial value for the age 561 Ma obtained by U-Pb dating of BB zircon. Individual analyses are reported in online supporting information.

Table 9.
Summary of results from SIMS oxygen isotope investigation

Reference material	Number of fragments/ grains analysed	Number of analyses	$\delta^{18}O$ SMOW (per mil, 1*s*)	Repeatability (per mil, 2*s*)	Published value for RM (2*s* uncert.)
91500	3	30	9.86[a]	0.24	9.86 ± 0.22 Wiedenbeck *et al.* (2004)
Penglai	2	20	4.91	0.26	5.31 ± 0.10 Li *et al.* (2010)
Plešovice	2	19	7.9	0.22	8.19 J.W. Valley (unpublished data)
Temora 2	14	21	7.97	0.34	8.2 Black *et al.* (2004)
BB9	3	31	13.5	0.56	This study
BB12	3	29	13.43	0.32	
BB25	2	19	12.74	0.34	
BB39	3	30	12.83	0.20	

All values reported in this table are simple means of the stated number of analytical results. [a] Zircon 91500 was used as the calibration material for determining the absolute $\delta^{18}O$ values of all other materials. Hence, its result is the assigned literature value.

Comparison with other Sri Lankan reference zircons and comments on origin

The relatively consistent chemical and physical properties of Sri Lankan zircons from gem gravels of the Ratnapura District (including their outstanding megacrystic size - of several mm) underlies the reasoning for their use as international intralaboratory reference materials. specifically, samples SL7 (Kinny *et al.* 1991), CZ3 (Pidgeon *et al.* 1994), M257 (Nasdala *et al.* 2008) and BR266 (Stern 2001) are in common use for Pb-U and/or Lu-Hf isotope determinations, especially for use with ion probe instruments. For laser ablation ICP-MS analysis, Gehrels *et al.* (2008) used a Sri Lankan zircon crystal as a primary age calibration material.

Ratnapura zircons, as a group, have high $\delta^{18}O$ values, values much greater than mantle values (~ 5.1‰, Valley 2003) and all above ~ 13‰ VSMOW (Vienna Standard Mean Ocean Water). This isotope feature indicates a significant surficial component was incorporated in the source rocks at the depth of crystallisation in either a metamorphic or igneous setting. Cathodoluminescence patterns are variable, from oscillatory zoning typically assigned to igneous types (Chakoumakos *et al.* 1987, Kröner *et al.* 1987) to broad, bland zoning ascribed to high-grade metamorphic zircons. Based on the high oxygen isotope ratios, Cavosie *et al.* (2011) proposed that these Ratnapura megacrysts must have a metamorphic origin, probably a marble or Ca-silicate skarn. Determining the

petrogenesis for BB zircons was not a specific goal of this paper, but a metamorphic origin appears likely.

SL7, CZ3, M257, BR266 and the Sri Lankan RMs of Gehrels *et al.* (2008) have average U contents of 2678, 551, 840, 909 and 518 μg g^{-1}, and Th/U ratios of 0.15 (Kinny *et al.* 1991), 0.06 (Pidgeon *et al.* 1994), 0.27 (Nasdala *et al.* 2008), 0.22 (Stern 2001) and 0.13 (Gehrels *et al.* 2008), respectively. In contrast, the BB zircons analysed herein have a U content range of 227–368 μg g^{-1} and Th/U ratios averaging 0.20–0.47 (for different grains). In addition, the SL7, BR266 and M257 show only small variations in their REE mass fraction compared with our data from the BB zircons; however, all of these materials show the same general REE pattern (steep chondrite-normalised patterns enriched in HREE relative to LREE, small negative Eu and positive Ce anomalies). This pattern is very different from patterns of a number of igneous zircons, such as M127 (Figure 13), and supports the interpretation of Cavosie *et al.* (2011), that the Ratnapura zircons are derived from a marble or Ca-silicate skarn. It is notable that all of the measured Th/U ratios, except CZ3, are significantly higher than 0.1, probably reflecting the composition of the source rock.

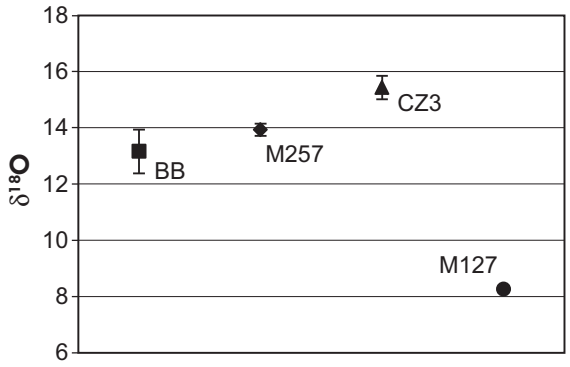

Figure 12. $\delta^{18}O$ SMOW values of BB, M257, CZ3 and M127 zircons.

Furthermore, these Sri Lankan zircon reference materials have very similar $^{206}Pb/^{238}U$ ages and $^{176}Hf/^{177}Hf$ values

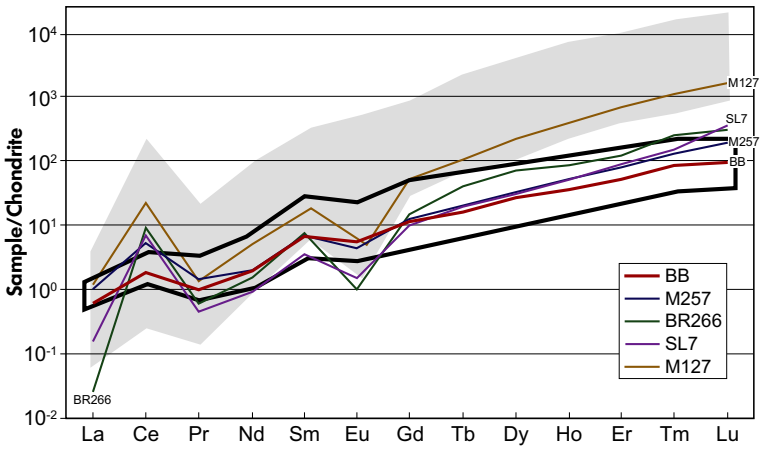

Figure 13. Chondrite-normalised grain rare earth element (REE) (average) composition of the BB, M257, BR266, SL7 and M127 zircons. The black line delimits the field for several analyses of BB zircons and the grey area indicates REE mass fraction ranges obtained for igneous zircon (graphically extracted from figure 4 in Hoskin and Schaltegger 2003 and figure 4 in Nasdala *et al.* 2016).

Table 10.
Summary of U-Pb age and Hf data for Sri Lankan zircons

Reference material	Age (± 1s, Ma)	$^{176}Hf/^{177}Hf$ (± 2s)	Reference
SL7	569 ± 3	0.28160 ± 0.00006[b]	Kinny *et al.* (1991)
CZ3	564 ± 2	0.281704 ± 0.000017[c]	Pidgeon *et al.* (1994), Xu *et al.* (2004)
BR266	559 ± 0.3	0.281624 ± 0.000024[c]	Stern (2001), Woodhead *et al.* (2004)
M257	561 ± 0.3	0.281544 ± 0.000018[c]	Nasdala *et al.* (2008), Hu *et al.* (2012)
Sri Lanka	564 ± 2		Gehrels *et al.* (2008)
BB9	561 ± 2[a]	0.281674 ± 0.000018[c]	This study

[a] $^{206}Pb/^{238}U$ ID-TIMS age of BB9 zircon; [b] TIMS Hf isotope analyses; [c] LA-MC-ICP-MS Hf.

(Table 10), also implying a common metamorphic history. The initial $^{176}Hf/^{177}Hf$ of the SL7, CZ3 and BB zircon corresponds to a ε_{Hf} of approximately -23.0 (Kinny *et al.* 1991), -25.5 (Xu *et al.* 2004) and -26.8 (this work), respectively, suggestive of a substantial crustal history.

Conclusions

The BB zircon crystals constitute a suitable reference material for LA-ICP-MS analysis of zircon. Based on a number of high-quality techniques, including ID-TIMS and LA-ICP-MS, we were able to demonstrate that the BB zircon is a suitable normalisation and quality control reference material for both U-Pb and Lu-Hf isotope systems, provided that analyses target pristine CL-dark grain domains. The homogeneous domains make up the majority of the crystals and can be easily separated from zones of fracture-controlled alteration and recrystallisation. Various megacrystals were tested in a number of LA-ICP-MS analytical set-ups and were shown to be concordant to somewhat normally discordant. Individual fragments of the BB zircons have minor U-Pb age variation (0.4% RSD) that is only detectable by ID-TIMS analysis and is within uncertainty of the age precision obtained with LA-ICP-MS (*ca.* 1–2%, 2*s*). The BB crystals are marked by very low levels of initial common Pb and high uranium and radiogenic lead mass fractions, yielding high count rates and good counting statistics. The LA-ICP-MS data from six different LA-ICP-MS laboratories (n = 635 points) gave mean ages of 564 ± 33 Ma (2*s*, $^{207}Pb/^{206}Pb$), 562 ± 9 Ma (2*s*, $^{206}Pb/^{238}U$) and 562 ± 10 Ma (2*s*, $^{207}Pb/^{235}U$). Using BB9 zircon as a reference material, and assuming mean TIMS ages reported in Table 6b, yields Concordia ages for a range of zircon reference materials within uncertainty of their published ages. We therefore conclude that the BB crystals perform well as either primary calibration or as quality control materials for LA-ICP-MS U-Pb geochronology and that the BB sample suite will be a useful addition to other materials available.

Laser ablation MC-ICP-MS analyses yielded low Lu/Hf (average of 0.00008) and Yb/Hf (average of 0.000005) ratios, which simplifies the task of isobaric interference correction, resulting in a better analytical uncertainty for the corrected $^{176}Hf/^{177}Hf$ ratios. The mean $^{176}Hf/^{177}Hf$ value of 0.281674 ± 0.000018 (2*s*) is considered the best estimate of the Hf isotope composition of the BB zircon and is valid for any random chip to be used as a reference sample.

Cathodoluminescence imaging shows a remarkably high degree of internal homogeneity for large parts of individual crystals. The same applies to some trace element mass fractions, as variations in chemical composition, determined by LA-ICP-MS analyses, did not exceed experimental uncertainties. Some fractured and resealed, CL-bright domains are, however, clearly depleted in some trace and REE elements and yield *ca.* 10 My younger U-Pb ages. Further analysis will be required to demonstrate that BB zircon can be used as a reference material for *in situ* REE determinations.

Finally, our SIMS results on the oxygen isotope ratio of the BB zircons have shown that the intergrain variations are fairly modest and the oxygen isotope heterogeneity with some of the single samples is small enough that these might in the future prove to be useful calibrants for $\delta^{18}O$ determinations by SIMS.

Acknowledgements

This work was funded by CNPq (projects 402852/2012-5, 401334/2012-0, 302633/2011-1, 305284/2015-0), FAPEMIG (projects CRA RDP00067-10, APQ03943 and APQ-01448-15), FINEP (project CT-INFRA) and PROPP/UFOP (03/2014 and 02/2015). We would like to acknowledge help from Adriana Tropia, José Cirilo Pereira and Antônio Celso Torres for assistance with laboratory preparation. Maristella Santos acknowledges scholarship from CAPES. ISB acknowledges support from the National Research Foundation (South Africa) and the CNPq (Science without Borders Program, Brazil). U. Dittmann and F. Couffignal played key roles in sample preparation and the subsequent analysis of the BB material for oxygen isotope systematics. We thank L. Nasdala and J. Sláma for providing reference materials M127 and Plešovice, respectively. Lastly, we would like to thank three anonymous reviewers for constructive comments and suggestions.

References

Batumike J.M., Griffin W.L., Belousova E.A., Pearson N.J., O'Reilly S.Y. and Shee S.R. (2008)
LAM-ICP-MS U-Pb dating of kimberlitic perovskite: Eocene-Oligocene kimberlites from the Kundelungu Plateau, D.R. Congo. **Earth and Planetary Science Letters, 267**, 609–619.

Black L.P., Kamo S.L., Allen C.M., Aleinikoff J.N., Davis D.W., Korsch R.J. and Foudoulis C. (2003)
TEMORA 1: A new zircon standard for Phanerozoic U-Pb geochronology. **Chemical Geology, 200**, 155–170.

references

Black L.P., Kamo S.L., Allen C.M., Davis D.W., Aleinikoff J.N., Valley J.W., Mundil R., Campbell I.H., Korsch R.J., Williams I.S. and Foudoulis C. (2004)
Improved $^{206}Pb/^{238}U$ microprobe geochronology by the monitoring of a trace-element related matrix effect; SHRIMP, ID-TIMS, ELA-ICP-MS and oxygen isotope documentation for a series of zircon standards. Chemical Geology, 205, 115–140.

Cavosie A.J., Valley J.W., Kita N.T., Spicuzza M.J., Ushikubo T. and Wilde S.A. (2011)
The origin of high $\delta^{18}O$ zircons: Marbles, megacrysts, and metamorphism. Contributions to Mineralogy and Petrology, 162, 961–974.

Chakoumakos B.C., Murakami T., Lumpkin G.R. and Ewing R.C. (1987)
Alpha-decay induced fracturing in zircon – The transition from the crystalline to the metamict state. Science, 236, 1556–1559.

Cherniak D.J. and Watson E.B. (2001)
Pb diffusion in zircon. Chemical Geology, 172, 5–24.

Cherniak D.J. and Watson B. (2003)
Diffusion in zircon. In: Hanchar J.M. and Hoskin P.W.O. (eds), Zircon. Reviews in Mineralogy and Geochemistry, 53, 113–143.

Crowley J.L., Schoene B. and Bowring S.A. (2007)
U-Pb dating of zircon in the Bishop Tuff at the millennial scale. Geology, 35, 1123–1126.

Dewaele S., Henjes-Kunst F., Melcher F., Sitnikova M., Burgess R., Gerdes A., Fernandez M.A., Clercq F., Muchez P. and Lehmann B. (2011)
Late Neoproterozoic overprinting of the cassiterite and columbite-tantalite bearing pegmatites of the Gatumba area, Rwanda (Central Africa). Journal of African Earth Sciences, 61, 10–26.

Dharmapriya P.L., Malaviarachchi S.P.K., Santosh M., Tang L. and Sajeev K. (2015)
Late-Neoproterozoic ultrahigh-temperature metamorphism in the Highland Complex, Sri Lanka. Precambrian Research, 271, 311–333.

Dissanayake C.B. and Rupasinghe M.S. (1993)
A prospector's guide map of the gem deposits of Sri Lanka. Gems and Gemmology, 29, 173–181.

Dissanayake C.B., Chandrajith R. and Tobschall H.J. (2000)
The geology, mineralogy and rare element geochemistry of the gem deposits of Sri Lanka. Bulletin of the Geological Society of Finland, 72, 5–20.

Gehrels G.E., Valencia V. and Ruiz J. (2008)
Enhanced precision, accuracy, efficiency, and spatial resolution of U-Pb ages by laser ablation-multicollector-inductively coupled plasma-mass spectrometry. Geochemistry, Geophysics, Geosystems, 9, Q03017.

Gonçalves G.O., Lana C., Scholz R., Buick I.S., Gerdes A., Kamo S.L., Corfu F., Marinho M.M., Chaves A.O., Valeriano C. and Nalini H.A. Jr (2016)
An assessment of monazite from the Itambé pegmatite district for use as U-Pb isotope reference material for microanalysis and implications for the origin of the "Moacyr" monazite. Chemical Geology, 424, 30–50.

Griffin W.L., Pearson N.J., Belousova E.A. and Saeed A. (2006)
Comment: Hf-isotope heterogeneity in zircon 91500. Chemical Geology, 233, 358–363.

Gulson B.L. and Jones M.T. (1992)
Cassiterite: Potential for direct dating of mineral deposits and a precise age for the Bushveld Complex granites. Geology, 20, 355–358.

Hölzl S., Hofmann A.W., Todt W. and Kiihler H. (1994)
U-Pb geochronology of the Sri Lankan basement. Precambrian Research, 66, 123–149.

Hoskin P.W.O. and Schaltegger U. (2003)
The composition of zircon and igneous and metamorphic petrogenesis. In: Hanchar J.M. and Hoskin P.W.O. (eds), Zircon. Reviews in Mineralogy and Geochemistry, 53, 27–62.

Hu Z., Liu Y., Gao S., Liu W., Zhang W., Tong X., Lin L., Zong K., Li M., Chen H., Zhou L. and Yang L. (2012)
Improved *in situ* Hf isotope ratio analysis of zircon using newly designed X skimmer cone and jet sample cone in combination with the addition of nitrogen by laser ablation multiple collector ICP-MS. Journal of Analytical Atomic Spectrometry, 27, 1391–1399.

Jackson S.E., Pearson N.J., Griffin W.L. and Belousova E.A. (2004)
The application of laser ablation-inductively coupled plasma-mass spectrometry to *in situ* U-Pb zircon geochronology. Chemical Geology, 211, 47–69.

Jaffey A.H., Flynn K.F., Glendenin L.E., Bentley W.C. and Essling A.M. (1971)
Precision measurement of half-lives and specific activities of ^{235}U and ^{228}U. Physical Review, C4, 1889–1906.

Jochum K.P., Weis U., Stoll B., Kuzmin D., Yang Q., Raczek I., Jacob D.E., Stracke A., Birbaum K., Frick D.A., Günther D. and Enzweiler J. (2011)
Determination of reference values for NIST SRM 610 – 617 glasses following ISO guidelines. Geostandards and Geoanalytical Research, 35, 397–429.

Kinny P.D., Compston W. and Williams I.S. (1991)
A reconnaissance ion-probe study of hafnium isotopes in zircons. Geochimica et Cosmochimica Acta, 55, 849–859.

Kröner A., Williams I.S., Compston W., Baur N., Vitanage P.W. and Perera R.K. (1987)
Zircon ion-microprobe dating of high-grade rocks in Sri Lanka. The Journal of Geology, 95, 775–791.

Kröner A., Jaeckel P. and Williams I.S. (1994a)
Pb-loss patterns in zircons from a high-grade metamorphic terrain as revealed by different dating methods: U-Pb and Pb-Pb ages for igneous and metamorphic zircons from northern Sri Lanka. Precambrian Research, 66, 151–181.

references

Kröner A., Kehelpannala K.V.W. and Kriegsman L.M. (1994b)
Origin of compositional layering and mechanism of crustal thickening in the high-grade gneiss terrain of Sri Lanka. Precambrian Research, 66, 21–37.

Li X.H., Long W.G., Li Q.L., Liu Y., Zheng Y.F., Yang Y.H., Chamberlain K.R., Wan D.F., Guo C.H., Wang X.C. and Tao H. (2010)
Penglai zircon megacrysts: A potential new working reference material for microbeam determination of Hf-O isotopes and U-Pb age. Geostandards and Geoanalytical Research, 34, 117–134.

Mattinson J.M. (2010)
Analysis of the relative decay constants of ^{235}U and ^{238}U by multi-step CA-TIMS measurements of closed-system natural zircon samples. Chemical Geology, 275, 186–198.

Morel M.L.A., Nebel O., Nebel-Jacobsen Y.J., Miller J.S. and Vroon P.Z. (2008)
Hafnium isotope characterization of the GJ-1 zircon reference material by solution and laser-ablation MC-ICP-MS. Chemical Geology, 255, 231–235.

Murakami T., Chakoumakos B.C., Ewing R.C., Lumpkin G.R. and Weber W.J. (1991)
Alpha-decay event damage in zircon. American Mineralogist, 76, 1510–1532.

Nasdala L., Reiners P.W., Garver J.I., Kennedy A.K., Stern R.A., Balan E. and Wirth R. (2004)
Incomplete retention of radiation damage in zircon from Sri Lanka. American Mineralogist, 89, 219–231.

Nasdala L., Hofmeister W., Norberg N., Martinson J.M., Corfu F., Dörr W., Kamo S.L., Kennedy A.K., Kronz A., Reiners P.W., Frei D., Košler J., Wan Y., Götze J., Häger T., Kröner A. and Valley J.W. (2008)
Zircon M257 – A homogeneous natural reference material for the ion microprobe U-Pb analysis of zircon. Geostandards and Geoanalytical Research, 32, 247–265.

Nasdala L., Corfu F., Valley J.W., Spicuzza M.J., Wu F., Li Q., Yang Y., Fisher C., Münker C., Kennedy A.K., Reiners P.W., Kronz A., Wiedenbeck M., Wirth R., Chanmuang C., Zeug M., Váczi T., Norberg N., Häger T., Kröner A. and Hofmeister W. (2016)
Zircon M127 – A homogeneous reference material for SIMS U-Pb geochronology combined with hafnium, oxygen and potentially, lithium isotope analysis. Geostandards and Geoanalytical Research, 40, 457–475.

Pidgeon R.T., Furfaro D., Kennedy A.K., Nemchin A.A. and Van Bronswijk W. (1994)
Calibration of zircon standards for the Curtin SHRIMP II. In: Eighth International Conference on Geochronology, Cosmochronology, and Isotope Geology – Abstracts: United States Geological Survey Circular, 1107, 251.

Sajeev K., Williams I.S. and Osanai Y. (2010)
Sensitive high-resolution ion microprobe U-Pb dating of prograde and retrograde ultrahigh-temperature metamorphism as exemplified by Sri Lankan granulites. Geology, 11, 971–974.

Santosh M., Tsunogae T., Malaviarachchi S.P.K., Zhang Z.M., Ding H.X., Tang L. and Dharmapriya P.L. (2014)
Neoproterozoic crustal evolution in Sri Lanka: Insights from petrologic, geochemical and zircon U-Pb and Lu-Hf isotopic data and implications for Gondwana assembly. Precambrian Research, 255, 1–29.

Schmitz M.D. and Schoene B. (2007)
Derivation of isotope ratios, errors and error correlations for U-Pb geochronology using ^{205}Pb–^{235}U–(^{233}U)-spiked isotope dilution thermal ionization mass spectrometric data. Geochemistry, Geophysics, Geosystems, 8, Q08006.

Schoene B., Crowley J.L., Condon D.J., Schmitz M.D. and Bowring S.A. (2006)
Reassessing the uranium decay constants for geochronology using ID-TIMS U-Pb data. Geochimica et Cosmochimica Acta, 70, 426–445.

Sláma J., Košler J., Condon D.J., Crowley J.L., Gerdes A., Hanchar J.M., Horstwood M.S.A., Morris G.A., Nasdala L., Norberg N., Schaltegger U., Schoene B., Tubrett M.N. and Whitehouse M.J. (2008)
Plešovice zircon – A new natural reference material for U-Pb and Hf isotopic microanalysis. Chemical Geology, 249, 1–35.

Speer J.A. (1982)
Zircon. In: Ribbe P.H. (ed.), Orthosilicates. Mineralogical Society of America Reviews in Mineralogy, 5, 67–l12.

Stern R.A. (2001)
A new isotopic and trace element standard for the ion microprobe: Preliminary TIMS U–Pb and electron microprobe data, current research. Radiogenic age and isotopic studies: Report 14. Geological Survey of Canada (Ottawa), 120pp.

Taylor S.R. and McLennan S.M. (1985)
The continental crust: Its composition and evolution. Blackwell (Oxford), 312pp.

Valley J.W. (2003)
Oxygen isotopes in zircon. In: Hanchar J.M. and Hoskin P.W.O. (eds), Zircon. Reviews in Mineralogy and Geochemistry, 53, 343–380.

Wiedenbeck M., Allé P., Corfu F., Griffin W.L., Meier M., Oberli F., von Quadt A., Roddick J.C. and Spiegel W. (1995)
Three natural zircon standards for U-Th-Pb, Lu-Hf, trace element and REE analyses. Geostandards Newsletter, 19, 1–23.

references

Wiedenbeck M., Hanchar J.M., Peck W.H., Sylvester P., Valley J.W., Whitehouse M.J., Kronz A., Morishita Y., Nasdala L., Fiebig J., Franchi I., Girard J.P., Greenwood R.C., Hinton R., Kita N., Mason P.R.D., Norman M., Ogasawara M., Piccoli R., Rhede D., Satoh H., Schulz-Dobrick B., Skar O., Spicuzza M.J., Terada K., Tindle A., Togashi S., Vennemann T., Xie Q. and Zheng Y.F. (2004)
Further characterisation of the 91500 zircon crystal. Geostandards and Geoanalytical Research, 28, 9–39.

Woodhead J.D. and Hergt J.M. (2005)
Preliminary appraisal of seven natural zircon reference materials for *in situ* Hf isotope determination. Geostandards and Geoanalytical Research, 29, 183–195.

Woodhead J.D., Hergt J.M., Shelley M., Eggins S. and Kemp R. (2004)
Zircon Hf-isotope analysis with an excimer laser, depth profiling, ablation of complex geometries and concomitant age estimation. Chemical Geology, 209, 121–135.

Xu P., Wu F.Y., Xie L.W. and Yang Y.H. (2004)
Hf isotopic compositions of the standard zircons for U-Pb dating. Chinese Science Bulletin, 49, 1642–1648.

ZhiChao L., Yuan W.F., ChunLi G., ZiFu Z., JinHui Y. and JinFeng S. (2011)
In situ U-Pb dating of xenotime by laser ablation (LA)-ICP-MS. Chinese Science Bulletin, 56, 2948–2956.

Supporting information

The following supporting information may be found in the online version of this article:

Appendix S1. Methodology.

Appendix S2. SEM images of mounted zircons.

Appendix S3. ID-TIMS U-Pb data for BB crystals.

Appendix S4. Hf isotope data for BB zircons.

This material is available as part of the online article from: http://onlinelibrary.wiley.com/doi/10.1111/ggr.12167/abstract (This link will take you to the article abstract).